



Fisheries and Oceans
Canada

Pêches et Océans
Canada

Ecosystems and
Oceans Science

Sciences des écosystèmes
et des océans

Canadian Science Advisory Secretariat (CSAS)

Research Document 2020/034

Quebec Region

A mechanistic approach to predicting suitable foraging habitat for reproductively mature North Atlantic right whales in the Gulf of St. Lawrence

Katherine Gavrilchuk¹, Véronique Lesage¹, Sarah Fortune², Andrew W. Trites², and Stéphane Plourde¹

¹ Fisheries and Oceans Canada
850 Route de la Mer, Mont-Joli, QC, CAN
G5H 3Z4

² University of British Columbia
2202 Main Mall, Vancouver, BC, CAN
V6T 1Z4

Foreword

This series documents the scientific basis for the evaluation of aquatic resources and ecosystems in Canada. As such, it addresses the issues of the day in the time frames required and the documents it contains are not intended as definitive statements on the subjects addressed but rather as progress reports on ongoing investigations.

Published by:

Fisheries and Oceans Canada
Canadian Science Advisory Secretariat
200 Kent Street
Ottawa ON K1A 0E6

[http://www.dfo-mpo.gc.ca/csas-sccs/
csas-sccs@dfo-mpo.gc.ca](http://www.dfo-mpo.gc.ca/csas-sccs/csas-sccs@dfo-mpo.gc.ca)



© Her Majesty the Queen in Right of Canada, 2020
ISSN 1919-5044

Correct citation for this publication:

Gavrilchuk, K., Lesage, V., Fortune, S., Trites, A.W., and Plourde, S. 2020. A mechanistic approach to predicting suitable foraging habitat for reproductively mature North Atlantic right whales in the Gulf of St. Lawrence. DFO Can. Sci. Advis. Sec. Res. Doc. 2020/034. iv + 47 p.

Aussi disponible en français :

Gavrilchuk, K., Lesage, V., Fortune, S., Trites, A.W., et Plourde, S. 2020. Une approche mécanistique à la prédiction de l'habitat favorable à l'alimentation des femelles sexuellement matures de baleine noire de l'Atlantique Nord dans le golfe du Saint-Laurent. Secr. can. de consult. sci. du MPO. Doc. de rech. 2020/034. iv + 50 p.

TABLE OF CONTENTS

ABSTRACT.....	iv
INTRODUCTION	1
MATERIALS AND METHODS	2
DATA COLLECTION.....	2
TWO-DIMENSIONAL PREY FIELD	2
THREE-DIMENSIONAL PREY FIELD.....	3
NET ENERGY FIELD.....	3
FORAGING BIOENERGETICS MODEL – ENERGY GAIN.....	4
FORAGING BIOENERGETICS MODEL – ENERGY EXPENDITURE	4
Basal metabolism.....	4
Travelling and foraging metabolism.....	5
Reproduction metabolism.....	7
FORAGING HABITAT SUITABILITY.....	8
RESULTS	8
DISCUSSION.....	10
PERSISTENT SUITABLE HABITAT IN THE GSL.....	10
VERTICAL DISTRIBUTION OF SUITABLE HABITAT.....	11
BIOENERGETICS.....	12
REFERENCES CITED.....	13
TABLES.....	22
FIGURES.....	27
APPENDIX.....	47

ABSTRACT

The North Atlantic right whale (*Eubalaena glacialis*, NARW) is an endangered cetacean which faces population decline from anthropogenic activities. Climate change may also be adding pressure on population recovery by shifting distribution of their preferred prey, *Calanus* copepods. The Gulf of St. Lawrence (GSL) in eastern Canada has been used as a foraging ground by a large proportion of the NARW population in recent years (at least from 2015 to present). Given the motivation to better understand NARW contemporary habitat use patterns and propose recovery measures for this population, we used a mechanistic modeling approach to predict areas that hold foraging potential in the GSL. We first assessed the overall annual energetic costs incurred by an adult female NARW in one of three reproductive states, and determined the theoretical prey densities required to sustain energy demand. We used a 12-year data set describing the abundance and three-dimensional distribution of late-stage *Calanus* copepods in the GSL coupled to a foraging bioenergetics model to identify potentially suitable foraging areas for NARW. Results show interannual variations in the spatial distribution and quantity of suitable habitat, with a decreasing amount of habitat available for resting, pregnant and lactating females, respectively. Suitable prey densities for foraging NARW were found in nearly all areas of the GSL that were surveyed for copepods, in one year or another, with a greater frequency of suitable prey densities identified in the southern GSL. Yearly maps of suitable foraging habitat for NARW were superimposed to identify areas that showed temporal persistence; the southern GSL (from Shediac Valley east to the Magdalen Islands) had suitable prey densities for all three reproductive states in most (≥ 6) years of the study period. For resting and pregnant females, other potential areas of foraging importance included offshore of Chaleurs Bay as well as the southern slope of the Laurentian Channel north of the Magdalen Islands. These findings highlight areas where NARWs may occur based on habitat modelled foraging value, and emphasize the need to survey offshore, under-studied regions in the GSL to better characterize NARW occurrence and habitat use patterns.

INTRODUCTION

The North Atlantic right whale (NARW; *Eubalaena glacialis*) is an endangered mysticete cetacean migrating along the east coast of Canada and the U.S. This population was estimated at 444 to 471 individuals in 2015, of which approximately 100 were sexually mature females (Pace et al. 2017). Population size has likely decreased since then given the continuing low birth rate and high mortality event documented in 2017 (Pettis et al. 2018). NARWs use Canadian and northern U.S. waters primarily to forage during the summer months, and use waters off southeastern U.S. for breeding and calving during the winter months (DFO 2014). Important prey have been identified as calanoid copepod species, mainly late-stage *Calanus finmarchicus*, *Pseudocalanus* spp. and *Centropages* spp., and potentially *C. glacialis* and *C. hyperboreus*, which have also been collected on NARW feeding grounds (Kraus and Prescott 1982; Murison and Gaskin 1989). Larval barnacles and euphausiids are also occasionally consumed (Watkins and Schevill 1976; Murison and Gaskin 1989; Mayo and Marx 1990). Right whales may be particularly vulnerable to inadequate prey densities given their specialized ram filter feeding strategy that relies on the environment to concentrate prey into compact, energetically profitable layers (Michaud and Taggart 2011).

Within Canada, the Grand Manan Basin in the Bay of Fundy and Roseway Basin on the western Scotian Shelf have been designated as part of NARW Critical Habitat (Brown et al. 2009; DFO 2014). However, since 2011, fewer NARWs have been observed within these traditional feeding areas, leading to an accrued international effort to find alternate foraging sites (Kraus et al. 2016; Pettis and Hamilton 2016). Over the last few decades, small numbers of NARWs have been reported on a regular basis in the Gulf of St. Lawrence (GSL). Sightings were mainly opportunistic and within coastal waters, where most nautical activities occur. Consequently, little is known regarding seasonal NARW distribution and habitat use within the GSL.

In an initial attempt to identify potentially suitable foraging areas for NARW in the GSL and elsewhere in eastern Canada, basic bio-energetic requirements for NARW were applied to a 3-D spatial climatology for *Calanus* species to help refine feeding areas identified based strictly on prey densities (Plourde et al. 2019). In this study, we brought this exercise one step further by incorporating it into an analysis considering interannual variations in the *Calanus* prey field the theoretical energy requirements for NARWs for adult females in one of three reproductive states derived from more complex and complete bio-energetics and bio-mechanics models. This type of model can be used to predict areas which may be of interest to a foraging predator, based on physiological and biomechanical principles shared by all organisms (Sibly et al. 2012; Peterson et al. 2015). The fundamental unit of measure in these mechanistic models is energy (expressed in Joules; J), and is referred to as the universal currency in ecology due to its direct influence on survival and reproduction (Stephens and Krebs 1986; McNab 2002).

From a reductionist perspective, the likelihood of an animal feeding at a given location reflects the trade-off between energy expended for energy gained, where animals are assumed to favor food items or foraging sites that provide a net energy gain in the long-term, in order to sustain life history functions and vital rates (Hall et al. 1992; Olsson and Bolin 2014). Given that reproductive status influences energy requirements (Sibly and Calow 1986), a particular habitat may not be equally suitable for all individuals in a population. To account for this, foraging habitat suitability in the GSL was modeled for adult females in three different reproductive states. Considering uncertainty about the main prey consumed by NARW in the GSL, the effect of feeding on different species of *Calanus* copepods or on other zooplankton species on habitat suitability was explored in a separate study using the bioenergetics modelling approach presented here (Lehoux et al. 2020).

MATERIALS AND METHODS

DATA COLLECTION

Ship-based, point-sampled zooplankton data has been collected in the Estuary and Gulf of St. Lawrence by Fisheries and Oceans Canada since 1979, providing a prey database with broad spatial and temporal coverage (Plourde et al. 2019). For this study, we selected sampling years with the most consistent spatial coverage in the GSL (2006 to 2017) during the summer season. Early summer surveys (June to early July) were primarily carried out in the southern GSL following a systematic design, while the late summer surveys (late July to Sept.) covered mainly the northern GSL and followed a random sampling design (Fig. 1).

The methodology for depth-integrated zooplankton sampling and determination of abundance (number of individuals m^{-2}) for the three dominant *Calanus* copepod species (*Calanus finmarchicus*, *C. glacialis* and *C. hyperboreus*) is summarized in Plourde et al. 2019; Sorochan et al. 2019). For this modeling exercise, we assumed that NARWs foraged on all three *Calanus* species, and on the later development stages (C4 to C6), for which their baleen has the highest filtration efficiency (Mayo et al. 2001). We grouped these stages and species to obtain a global *Calanus* copepod biomass and distribution measure in the GSL following Plourde et al. (2019).

TWO-DIMENSIONAL PREY FIELD

A continuous prey field was first generated using Bayesian geostatistical inference to predict depth-integrated *Calanus* biomass (g DW m^{-2}) at unsampled locations in the GSL for both early and late summer of each year (e.g. Cosandey-Godin et al. 2014; Nikolioudakis et al. 2018). We used continuous domain stochastic partial differential equations (SPDE) to solve the covariance structure of *Calanus* biomass observations (Lindgren et al. 2011) using the R package [R-INLA](#).

Our response variable (*Calanus* biomass) was positive-continuous with a small percentage (1%) of zeros. To avoid removing the zero data, we chose to add a negligibly small value (0.001) to the zeros and evaluated the goodness of fit of three candidate distributions (gamma, exponential and lognormal). We included potential static (bathymetry and slope) and dynamic (sea surface temperature) environmental correlates of copepod abundance and distribution to explore their utility for informing predictions. Bathymetry (m) and slope ($^{\circ}$) data were obtained for each sampling station in the GSL from the satellite-derived, high-resolution (1 km^2 grid) [MARSPEC](#) database, which uses data from NOAA's World Ocean Atlas and NASA's MODIS satellite imagery. Daily SST data was extracted via the ERDDAP data server from the Multi-scale Ultra-high Resolution (MUR, 1 km^2) SST Global database (NASA JPL).

We let $y(s_i)$ denote the realization of the spatial process $Y(\cdot)$, which represents the mean *Calanus* biomass measured at station i at location s_i ,

$$y(s_i) = z(s_i)\beta + w(s_i) + \varepsilon(s_i)$$

where $z(s_i)$ is the vector of covariate values for location s_i , β is the vector of regression coefficients, $w(s_i)$ is the spatial random effect which addresses spatial autocorrelation in the data, and is represented by a continuously indexed Gaussian Field with Matérn covariance structure (Gaussian Markov Random Field; Lindgren et al. 2011), and $\varepsilon(s_i) \sim N(0, \sigma^2_{\varepsilon})$ is the spatially uncorrelated measurement error (Cameletti et al. 2013). All covariates were included as smoothed (varying) effects given the non-linear relationships observed with the response variable during data exploration. All covariates were standardized to avoid numerical estimation issues and to facilitate interpretation of regression parameters. The model was run for each year and season (early, late summer) separately to obtain *Calanus* biomass prey field predictions for all 12 years. A spatio-temporal modeling framework could also be used with this dataset, if the

interest is to predict *Calanus* prey fields in future, while accounting for temporal autocorrelation in the time series.

Under the Bayesian paradigm, model parameters are considered random variables and defined using prior probability distributions. For the smoothed (non-linear) effect of the covariates, we assigned a first-order random walk model (Cosandey-Godin et al. 2014; Krainski et al. 2017) with penalized complexity (PC) prior probability distributions recommended by Simpson et al. (2017); where the probability of the prior's standard deviation (σ) being greater than 1 is 0.05. For the spatial random effect, we set PC priors for the spatial correlation range r and the standard deviation σ so that $P(r < 10) = 0.05$ and the $P(\sigma > 3) = 0.05$ (Fuglstad et al. 2018).

We compared various candidate models (all additive covariate combinations) fitted with and without the spatial random effect using the Deviance Information Criterion (DIC; Spiegelhalter et al. 2002) and the Watanabe-Akaike Information Criterion (WAIC; Watanabe 2010), where the lower the DIC or WAIC value, the higher the goodness of fit. Two additional cross-validation methods were used to assess predictive performance of candidate models. We first randomly selected 80% of the data for model estimation and 20% for validation to evaluate how well the model predicted *Calanus* biomass at validation locations using the correlation between observed and predicted *Calanus* biomass. We then used the built-in R-INLA leave-one-out cross-validation diagnostic (the conditional predictive ordinate, CPO), which calculates a prediction error score for each observation. To summarize CPO values for all observations into one metric, the sum of all log CPO values was computed, in which larger values indicate better model predictive power (Gneiting and Raftery 2007).

The final model was used to predict depth-integrated *Calanus* biomass on a 10 x 10 km regular grid covering the study area in early summer (mid-June) and late summer (mid-August) for each year in the study period. We extended predictions up to a maximum distance of 30 km from sampling sites to reduce uncertainty. Covariate values at prediction locations were obtained the same way as for the observed *Calanus* data.

THREE-DIMENSIONAL PREY FIELD

The seasonal vertical distribution of *Calanus* copepods in the northwest Atlantic was assessed in a preceding study using depth-stratified *Calanus* abundance data and a generalized additive modeling approach (Krumhansl et al. 2018, Plourde et al. 2019). The resulting models predict the daily averaged *Calanus* copepod biomass density (g m^{-3}) in 10 m depth intervals from surface to sea floor. Given the available data, these vertical distribution models were built on a relatively coarse temporal (seasonal and regional resolution), and therefore do not capture the diel vertical migration of *Calanus* in early summer (Plourde et al. 2019). We applied the *Calanus* vertical distribution models to our two-dimensional (2D) 10 km² grid of predicted depth-integrated *Calanus* biomass to produce a three-dimensional (3D) representation of the prey field.

NET ENERGY FIELD

From the 3D prey field, we extracted two parameters for the foraging bioenergetics model (described below) – *Calanus* biomass density predicted in 10 m depth layers, and the depth of each layer or transit distance from the water surface to access prey. The foraging bioenergetics model was then applied to the 3D prey field to obtain a 3D net energy field, where each xyz location (latitude-longitude-depth) was assigned a net energy index (E_{net}) according to a simple theoretical energy balance,

$$E_{\text{net}} = \frac{E_{\text{in}} - E_{\text{out}}}{E_{\text{out}}}$$

where E_{net} is the proportion of energy gained (E_{in}) or expended (E_{out}), relative to energy expended (E_{out}). An E_{net} value of zero signifies that energy gained equals energy expended. For this study, we considered $E_{\text{net}}=0$ as the minimum theoretical foraging threshold. Any xyz locations with E_{net} values > 0 were defined as “suitable” for meeting NARW daily energy requirements, according to the foraging assumptions made below. Values for certain model parameters are summarized in Table 1.

FORAGING BIOENERGETICS MODEL – ENERGY GAIN

Right whales feed by ram filtration, which involves passively filtering large volumes of prey-filled water by slowly swimming forward with mouth open (Mayo and Marx 1990). The volume of prey-water filtered per unit time can be used to approximate the rate of energy gain (E_{in}) in MJ day^{-1} (Baumgartner and Mate 2003),

$$E_{\text{in}} = (A_m U_b T_b E_p D_p) \varepsilon_A$$

where A_m (m^2) is mouth opening area, U_b (m s^{-1}) is foraging swim speed, T_b (s day^{-1}) is time spent ingesting prey, E_p (MJ g^{-1}) is prey energy content, D_p is prey density (g m^{-3}), and ε_A is dietary assimilation efficiency, or the ratio of energy gained after digestion to energy ingested (Table 1).

FORAGING BIOENERGETICS MODEL – ENERGY EXPENDITURE

We evaluated the annual ‘cost of living’ for an adult female NARW in either a resting, pregnant or lactating state that forages during the summer, breeds or calves in the winter, and migrates during the fall and spring. Using available literature on the general activity budget of NARWs, we assumed the following: during each season, the proportion of time spent in three principal activities (foraging, travelling and socializing, resting) varies. Foraging is the dominant activity during the summer, travelling is the dominant activity during the fall and spring migrations, and travelling and socializing is the main activity during winter (see Table 2 and references therein). Given the variability in swimming parameters and body kinematics during social activity, as well as the uncertainty in how to quantify associated energetic expenditure, we grouped travelling and socializing behaviour into one category and assumed our estimates of travel metabolism captures both behaviours. Foraging was assumed negligible during migration and while on the wintering grounds (Winn et al. 1986). The resulting daily energy expenditure (E_{out} , MJ day^{-1}) was calculated for each reproductive state k (resting, pregnant or lactating) as:

$$E_{\text{out}_k} = \frac{\sum_{i=1}^n \sum_{a=1}^n T_{ai} \cdot M_a + E_{\text{repro}}}{T_f}$$

where i is the season ($n = 4$; winter, spring, summer, fall), a is the activity type ($n = 3$; foraging, travelling and socializing, resting), T_{ai} is the number of daily hours spent on activity a during season i , M_a is the activity-specific energy cost, E_{repro} is the energy required for gestation or lactation per year, and T_f is the number of days spent foraging per year, inferred from observed NARW migration time and residency on wintering grounds (Table 2).

Basal metabolism

For marine mammals, the basal metabolic rate (BMR) is difficult to measure under Kleiber standards (e.g. ensuring individuals are motionless and thermoneutral) and is often referred to as resting metabolic rate (RMR) instead. The following allometric RMR relationship is specific to

marine mammals (Williams and Maresh 2015), and is comparable to Kleiber (1975)'s widely-used BMR equation (95% of BMR).

$$\text{RMR} = 581\text{mass}^{0.68}$$

where body mass is in kg, and RMR is in kJ d^{-1} (converted to MJ). An average body mass of 35,000 kg was used for a 14-m long NARW (Moore et al. 2005).

Travelling and foraging metabolism

The cost of travelling and foraging was estimated using published morphometric and kinematic parameters for NARWs (Baumgartner and Mate 2003; Nousek McGregor 2010; Nousek-McGregor et al. 2014; van der Hoop et al. 2013; van der Hoop et al. 2016). There are four main forces acting on pelagic swimming species: weight, buoyancy, propulsion (or thrust) and drag; where weight counteracts buoyancy and propulsion counteracts drag (Tucker 1975; Schmidt-Nielsen 1997). The buoyancy force fluctuates with individual body condition, which can cycle through periods of higher buoyancy during blubber accumulation and lower buoyancy during blubber breakdown/catabolism (Miller et al. 2012a; Nousek-McGregor et al. 2014). To quantify the buoyancy force, data on animal blubber volume, tissue density, and volume of gas-filled cavities are required (Miller et al. 2004; Sato et al. 2010). Since this information was unavailable, we assumed that for the positively-buoyant right whale (Nowacek et al. 2001), energy expended to overcome buoyancy during dive descent is balanced by energy savings during ascent (Hays et al. 2007), and focused on the propulsion and drag components of movement metabolism.

The propulsive power (P_p , J s^{-1}) required for travelling and foraging was calculated using standard physics and biomechanics equations, which can be applied to any species or moving body and multiplied by the estimated time (s) spent in each activity per day (Table 2) to quantify daily activity costs (J day^{-1}). Propulsive power is a function of the hydrodynamic drag force (F_{drag} , N), swim speed (U m s^{-1}), and energy transfer efficiency – a combination of muscular (or metabolic) efficiency (η_m) and propulsive (or propeller) efficiency (η_p). Right whales modulate their swim speed with behaviour, and even within different phases of a foraging dive (descent, bottom, ascent and surface recovery). Thus, P_p was calculated separately for travelling and for each foraging dive phase,

$$P_p = \frac{F_{\text{drag}}U}{\eta_m \eta_p}$$

where the magnitude of the drag force (F_{drag}) depends on swim speed, body form, characteristics of the surrounding medium, proximity to boundaries such as the air-water interface, and the relative contribution of inertial, viscous, and gravitational forces (Fish 1998). F_{drag} on a moving right whale can be calculated as,

$$F_{\text{drag}} = \frac{1}{2} \rho C_D A U^2 g \lambda \gamma$$

where ρ is the density of the surrounding medium (seawater), C_D is the dimensionless drag coefficient, and A is the total wetted surface area (m^2), which can be approximated using an allometric relationship to body mass (Table 1). The surface area A was increased by 5% for pregnant females based on aerial photogrammetric measurements and blubber thickness data (Nousek McGregor 2010). U is the swim speed (m s^{-1}), g is the added drag of appendages (flukes and flippers), λ is the active-to-passive drag ratio, and γ is surface wave drag augmentation factor. For the latter two, body oscillation during active locomotion alters the hydrodynamic and drag regime around a moving body and is quantified using the active-to-

passive drag ratio (λ). There is uncertainty whether active swimming increases or decreases overall drag relative to passive gliding in swimming animals (Williams and Kooyman 1985; Fish et al. 1988; Fish 1993; Hind and Gurney 1997; Barrett et al. 1999; Borazjani and Sotiropoulos 2008). Given the lack of consensus for this value, we assume a conservative $\lambda = 1.0$, comparable to previous bioenergetic studies on marine mammals (Aoki et al. 2011; Miller et al. 2012b; Trassinelli 2016). Surface wave drag (γ) affects animals swimming at or near the water surface (Vogel 1994), and gradually decreases with depth, becoming negligible ($\gamma = 1$) at submergence depths greater than three times the maximum body diameter (Hertel 1969). Given the uncertainty regarding the influence of surface wave drag on NARW energy expenditure, we set $\gamma = 1$ for this model.

The drag coefficient (C_D) of the above F_{drag} equation was calculated by multiplying the skin friction coefficient (first expression in parentheses below) by the body dimensions, also known as the ‘form factor’ (second expression in parentheses; Phillips et al. 2017),

$$C_D = (\alpha \text{Re}^\beta) \cdot \left(1 + 1.5 \left(\frac{L}{d} \right)^{-\frac{3}{2}} + 7 \left(\frac{L}{d} \right)^{-3} \right)$$

where L is the body length, d is the maximum body diameter, and Re is the Reynold’s number (Reynolds 1883), which describes the flow regime around a body of length L moving at speed U (m s^{-1}) through a medium with kinematic viscosity ν (Table 1),

$$\text{Re} = \frac{LU}{\nu}$$

At high Reynold’s numbers ($>5 \times 10^6$), which is the case for right whales given their body size and typical swim speed, fluid flow around the body transitions from laminar to turbulent, increasing the value of the skin friction coefficient (Kline et al. 1967). Under a turbulent flow regime, the skin friction component of the drag coefficient (C_D) can be calculated using the constant $\alpha = 0.072$ and the exponent $\beta = -0.2$ (von Kármán and Millikan 1934).

The drag force acting on a NARW during foraging is greater than during travelling since open-mouth feeding exposes a larger surface area to oncoming water flow, adding resistance to forward motion (Sanderson and Wassersug 1990; Potvin and Werth 2017). For a given speed, foraging increases drag by an estimated 2 to 3 times compared to travelling in NARWs (Nousek McGregor 2010; Potvin and Werth 2017). F_{drag} was thus multiplied by 2 and 3 to obtain low and high estimates of energy expended during foraging.

Most deep-diving marine mammals use an intermittent swimming gait, where active stroking is followed by periods of passive gliding; certain species also increase time spent gliding during descent on deeper dives (Williams et al. 2000). On a foraging dive, NARWs passively glide for an average 36% of descent time (range 10–75%), 30% of ascent time (20–36%), and 9% of bottom time (6–12%; Nowacek et al. 2001; Nousek McGregor 2010; Nousek-McGregor et al. 2014). The proportion of time NARWs spend gliding during surface recovery and during travelling is not known, but we assumed a similar glide time as during horizontal swimming during bottom phase (9%). We used average glide times and kept the proportion of time spent gliding in each phase constant with depth, as it is unknown how glide times vary with dive depth in NARWs. If the only energy expended during a passive glide is RMR, the total cost (J ; converted to MJ) of travelling per day can be approximated as,

$$E_{\text{travel}} = P_{\text{travel}} \cdot t_{\text{travel}} \cdot (1 - t_{\text{glide}})$$

and the total cost (J ; converted to MJ) of foraging per day at depth i is,

$$E_{\text{forage}_i} = \left[\sum_{j=1}^n Pp_j \cdot t_j \cdot (1 - t_{\text{glide}_j}) \right] \cdot n_{\text{dives}}$$

where j is one of four dives phases, Pp_j is the propulsive power (J s^{-1}) during dive phase j , t_{travel} and t_j are the times (s) spent travelling per day or in dive phase j per dive, t_{glide} is the proportion of time spent gliding, and n_{dives} is the theoretical maximum number of dives per day at a given depth if foraging ~ 15 to 17 h day^{-1} (Table 2), which would equate to daily ingestion times of ~ 5 to 10 h day^{-1} , depending on reproductive state, daily foraging time, and foraging depth. This is in accordance with an average daily ingestion time of 8.4 h day^{-1} reported from NARW tagging studies (Goodyear 1996).

Time (s) spent in ascent and descent phase was calculated as distance travelled (m) divided by swim speed (m s^{-1}) for each phase, where distance travelled is equal to dive depth (m) corrected for average body pitch (θ). During foraging dives, adult female NARWs pivot their body to around $69\text{--}78^\circ$ relative to the water surface on descent and $56\text{--}68^\circ$ relative to the sea floor on ascent, depending in part on body condition (Nousek-McGregor et al. 2014). We used average decent and ascent angles of 74° and 62° , respectively and calculated distance travelled during descent or ascent phase as,

$$\sin\theta_{\text{descent or ascent}} = \frac{\text{Depth}}{\text{Distance}}$$

Time spent in the bottom phase (t_b) for dive depths of 0 to 150 m was calculated according to Baumgartner et al. (2017)'s equation derived from NARW tagging studies,

$$t_b = 0.0704 \cdot \text{depth}$$

Bottom time for dive depths of 160 to 500 m was assumed constant and equal to the maximum bottom time predicted by the previous equation ($t = 636 \text{ s}$). Time spent in the surface phase (t_s) was expressed as a percentage of the total time spent at depth (Dolphin 1987; Thompson and Fedak 2001) and was assigned an average value of 21.1% and 34.2% for resting and pregnant/lactating females, respectively (Baumgartner and Mate 2003).

Reproduction metabolism

The gestation period for NARWs is about 12 months (Knowlton et al. 1994). During this time, females allocate energy to fetal, uterine, placental, and mammary tissue growth (Slijper 1966; Lockyer 1984). Following parturition, mothers need energy to produce milk to provision their young until weaning. The maternal energy required for gestation is correlated allometrically with newborn body mass, and this relationship has been used in several studies on cetacean energetics (e.g. Brodie 1975; Lockyer 1981, 2007; Fortune et al. 2013; New et al. 2013; Rechsteiner et al. 2013; Villegas-Amtmann et al. 2015),

$$H_g = 4400 \text{mass}_{\text{nb}}^{1.2}$$

where H_g is the heat increment of gestation (in kCal, converted to MJ using $1 \text{ kCal} = 0.004184 \text{ MJ}$), and M_{nb} is newborn mass (kg).

The energetic cost of lactation is a combination of both mother and calf metabolism (Lockyer 1981). The nursing period for large mysticetes is around 6–7 months (Ofstedal 1997) and NARW mothers and calves remain together for 8–17 months (Hamilton et al. 1995; Hamilton and Cooper 2010). Baumgartner and Mate (2003) report calves likely feeding on zooplankton at 8 months old. The cost of lactation was estimated by adding the average daily energy requirement of the calf ($1767 \pm \text{SD } 261 \text{ MJ}$; Fortune et al. 2013) to the daily energy requirement for a

lactating female, accounting for a milk transfer efficiency of 90% (Lockyer 1981). We assumed mothers provided 110% of the calf's daily energy requirements for the first 6 months after birth, followed by a linear decline in energy contribution (representing the gradual weaning period) up until 12 months, at which point the calf is presumed to feed independently (New et al. 2013).

FORAGING HABITAT SUITABILITY

We converted the 3D net energy field into a foraging habitat suitability grid for each year and reproductive state, as well as for all years combined. We first summed the number of depth layers with E_{net} values greater than zero (where zero is defined as energetic equilibrium) for each grid cell, then divided by the total number of depth layers per grid cell. This provided a relative and weighted measure of foraging value per cell with a value of 1.0 signifying that 100% of the water column was predicted to have suitable prey densities. We then built composite maps by stacking all 12 habitat suitability maps together and counting the number of years each 10 km² grid cell had a positive foraging value (comparable to Nelson et al. 2009). This provided information on which areas in the GSL showed temporally persistent suitable habitat. See Table 3 for an overview of all methodological steps. Note that "suitable habitat" in this document refers to any xyz location within the GSL with prey density that exceeds the theoretical daily energy requirements for adult female NARWs.

RESULTS

A total of 1543 stations were sampled for *Calanus* spp. abundance from 2006 to 2017 in the Estuary and Gulf of St. Lawrence (early season sampling only for 2016; Fig. 1, Table 4). Depth-integrated *Calanus* spp. biomass (CIV to CVI) ranged from 0–507.4 g dry weight (DW) m⁻² (median 2.5) and 0–244.9 g DW m⁻² (median 20.4) in early and late summer, respectively. INLA predictions of depth-integrated *Calanus* biomass at the 10km² grid locations are summarized in Table 5 from 2006 to 2017. The vertical distribution model predicted *Calanus* biomass density in 10-m depth layers from surface to sea floor with values ranging from 0–6.0 g DW m⁻³ (median: 0.2, mean: 0.5, SD: 0.6) in early summer, and values ranging from 0–5.8 g DW m⁻³ (median: 0.1, mean: 0.1, SD: 0.2) in late summer.

The gamma distribution outperformed the exponential and lognormal distributions for the early season data, and all three distributions were comparable in terms of model fit and predictive performance for the late season data. The gamma distribution was chosen for prediction with the best fitting model, which included additive smoothed effects of SST, slope, bathymetry and the spatial random effect. Using the estimation and validation data subsets, observed depth-integrated *Calanus* biomass values were correlated to predicted values with a mean \pm SD of 0.61 ± 0.11 in early season and 0.69 ± 0.10 in late season. Sea surface temperature and slope did not have a significant effect on *Calanus* biomass in early or late season (95% confidence intervals overlapped zero in all years). Bathymetry had little effect on *Calanus* biomass values in early season, and a positive effect in late season (Fig. 2 and 3). Over the 12-year study period, *Calanus* biomass values were spatially correlated up to a mean range of 71–434 km (median: 219, mean: 202, SD: 106) in early season, and 53–1642 km (median: 133, mean: 376, SD: 506) in late season, signifying a strong inter-annual variability in spatial correlation. The mean and SD of the spatial random effect for each year is shown in Fig. 4 and 5.

Annual energy expenditure (MJ day⁻¹) estimated for a 14 m-long adult female NARW in either a resting, pregnant or lactating reproductive state is summarized Table 6, and comparable to NARW energetic requirements estimated in previous studies (Fortune et al. 2013: 1013–5738 MJ day⁻¹; Baumgartner and Mate 2003; 1659 MJ day⁻¹; and closer to the lower range of Kenney et al. 1986's estimates: 1703–1732 MJ day⁻¹). Although adult males were not included in this

study, they require around 6% less energy (MJ d^{-1}) than resting adult females due to differences in body composition and lower residency times on breeding grounds which may allow males to spend more days per year on feeding grounds, lowering their overall daily energy requirements (Fortune et al. 2013). Assuming right whales spend $15\text{--}17 \text{ h day}^{-1}$ foraging during the summer, Fig. 6 shows the predicted daily ingestion time (h) if foraging at depths from 0 to 500 m, and the minimum predicted prey density requirement as a function of depth for each reproductive state. Prey densities required to meet daily energy output ranged from 0.62 to 2.67 (median 1.34) g m^{-3} for resting females; from 0.79 to 3.72 (median 1.80) g m^{-3} for pregnant whales; and from 1.82 to 8.48 (median 4.11) g m^{-3} for lactating whales. The depths associated with maximum E_{net} values ($\geq 98^{\text{th}}$ percentile) for all three reproductive states were 50m (median) in the early summer, and 220m in late summer. These depths coincided with maximum *Calanus* densities (50 m in early summer, and 230 m in late summer). The total percentage of E_{net} values exceeding zero within the 3D *Calanus* prey field was low; ranging from 1.0 to 6.5% for resting females, 0.5 to 4.7% for pregnant, and 0.01 to 0.9% for lactating females.

Predicted suitable foraging habitat for NARW in the GSL is presented in Figs. 7–15 for adult female NARW in three reproductive states. Figures 7–12 show predicted suitable habitat for each year in the study period. Figures 13–15 are composite maps of all years stacked together showing temporal persistence of suitable habitat, or the number of years (0 to 12) that a given grid cell had at least one depth layer with prey densities exceeding daily energy requirements for adult female NARW. Refer to Fig. S1 for place names, and to Fig. 1 for spatial distribution of sampling effort over the study period, keeping in mind the temporal and spatial effort bias within the GSL over the course of the summer season.

The minimum predicted suitable foraging habitat for resting NARW (Fig. 7) highlighted the southern GSL early in the time series (2006–2009), where after suitable habitat became progressively sparse through to 2017. In 2015, the only grid cells showing suitable prey densities were within the Strait of Belle Isle. Maximum predicted suitable habitat for resting females (Fig. 8) showed a consistent pattern of suitable prey densities in the southern GSL from 2006–2009, 2011–2014, 2016 and 2017, although the spatial configuration and magnitude of which differed from year to year. In 2010, the only grid cells with suitable prey densities for resting females appeared on the southern slope of the Laurentian Channel, north of the southern GSL (sGSL). Habitat with suitable prey densities varied spatially and among years in the northern GSL; for instance, in 2008 and 2009 suitable prey densities were spread in patches from the Estuary to Anticosti Island, and to the west of Newfoundland. In comparison, 2007, 2013, and 2014 had fewer grid cells showing suitable prey densities, which were mostly scattered along the north shore of the GSL (north of Anticosti) and into the northeast GSL, west of NFLD. Under maximum foraging conditions for resting females, several areas within the sGSL had $\geq 50\%$ of the water column with suitable prey densities in multiple years; these areas included Chaleurs Bay, Shediac Valley and surrounding waters, the southern slope of the Laurentian Channel north of the sGSL, waters off the Gaspé Peninsula and around the Magdalen Islands, and the middle of the Magdalen Shallows.

Similar patterns in the spatial distribution of suitable habitat were found for pregnant females under minimum and maximum foraging conditions (Fig. 9, 10). Years 2010, 2013, and 2015–2017 had little to no suitable prey densities under minimum conditions, except a few grid cells along the southern slope of the Laurentian Channel (2013, 2016), and within the Strait of Belle Isle (2015).

Under minimum conditions, only three years (2006, 2007, 2011) had suitable prey densities, albeit a very low number of grid cells, for lactating females (Fig. 11). Maximum predicted suitable habitat for lactating females was largely concentrated in the sGSL (2006–2009, 2011, 2012, 2014; Fig 12), with $\geq 50\%$ of the water column showing suitable prey densities in the

Shediac Valley area, around the Magdalen Islands, occasionally along the northwest tip of Prince Edward Island, and south of Miramichi Bay. Years 2010 and 2015–2017 were relatively poor years for habitat suitability even under maximum conditions for lactating females.

For resting females, the temporal persistence maps highlight the sGSL as a broad area with suitable prey densities in 6 or more years. Areas with over 10 years of consistently suitable prey densities were found at the entrance of Chaleurs Bay and along the southern slope of the Laurentian Channel, at the mid-GSL level (Fig. 13). Similar patterns were found for pregnant females (Fig. 14), and for lactating females (Fig. 15) under maximum foraging conditions. Areas showing 5 to 7 years of suitable prey densities for lactating females were located off Miramichi Bay/Shediac Valley region, spread across the Magdalen Shallows towards the Magdalen Islands.

DISCUSSION

PERSISTENT SUITABLE HABITAT IN THE GSL

We used a bottom-up approach to predict suitable foraging habitat for endangered North Atlantic right whales within the Gulf of St. Lawrence over a 12-year period (2006 to 2017). Based on theoretical energy requirements for adult female NARW in either a resting, pregnant or lactating reproductive state, we predicted the occurrence of suitable *Calanus* copepod densities primarily in the southern GSL. These results are consistent with predictions issued from a 3-D spatial climatology of *Calanus* preyscape, and to which simple NARW bio-energetic considerations were applied (Plourde et al. 2019). Our study showed that the total number of 10 km² grid cells with suitable prey densities and their spatial configuration varied among years. Several areas identified as potentially suitable foraging habitat for female NARWs due to temporal persistence (i.e., showing suitable prey densities in ≥ 5 years) were also identified using the shorter time series for *Calanus* distribution and densities, and the simpler bio-energetic approach (Plourde et al. 2019); some of them also corresponded to previously defined 'Ecologically and Biologically Significant Areas' (EBSAs) due to their biodiversity, productivity and uniqueness (DFO 2007). These include western Cape Breton, Northumberland Strait (between New Brunswick and Prince Edward Island), the southern slope of the Laurentian Channel, and the south-western coast of the GSL. Other EBSAs mirrored areas where suitable foraging habitat for NARW was predicted in a lower number of years (< 5), including the St. Lawrence Estuary, the Strait of Belle Isle, waters the north of Anticosti Island, and to the west of Newfoundland.

The southern GSL bathymetry is dominated by a broad, shallow shelf known as the Magdalen Shallows, which vary in depth from 60 to 80 m. North of the sGSL, the bathymetry abruptly changes to a steep submarine valley (the Laurentian Channel), which can reach depths of 500 m, traversing the GSL from Cabot Strait all the way to the Lower St. Lawrence Estuary. The southern slope of the Laurentian Channel situated north of the Magdalen Shallows is an important feeding, migration and shelter area for several fish species (e.g. Atlantic herring, capelin, white barracudina, spiny dogfish, pollock and silver hake; DFO 2009). Large aggregations of phytoplankton and zooplankton have occasionally been observed in this area, which may be an important wintering habitat for zooplankton (DFO 2007; Lavoie et al. 2007). The shallower sea floor of the sGSL likely acts as a physical barrier constraining the vertical distribution of *Calanus*, compacting them near the sea floor (Kaartvedt 1996; Krumhansl et al. 2018). In fact for any given water column biomass (mg m⁻²), the maximum *Calanus* biomass density (mg m⁻³ in 10-m depth layers) at a 60 m deep station (southern GSL) would be 5-6 times greater than at a 300 m location in the deep Laurentian Channel (Plourde et al. 2019). A combination of compressed *Calanus* layers and shorter dive distance to access these layers

may offer favorable foraging conditions for NARWs, and could explain why such a broad area of the sGSL showed suitable prey densities across multiple years.

Some of the densest euphausiid (krill) aggregations in the GSL have also been found in areas where we predicted NARW suitable foraging habitat (Maps et al. 2015; Plourde et al. 2016). Maps et al. (2015) used an extensive hydroacoustic krill survey dataset coupled to a dynamic particle trajectory model to demonstrate how certain mesoscale zones within the GSL tend to accumulate krill during the summer. These areas include the Lower St. Lawrence Estuary, waters south of Anticosti Island, the northeast GSL where the Esquiman and Anticosti channels bifurcate, as well as along borders of deep channels. Over one third of the highest krill aggregations have been located along the western shelf of Newfoundland (Maps et al. 2015), an area where we predicted suitable *Calanus* densities. However, a parallel study examining habitat suitability using the same bio-energetics model for NARW indicates that euphausiids are unlikely to be an important prey for NARW in the GSL given the low capture efficiency of NARW when feeding on this particular prey (Lehoux et al. 2020)

VERTICAL DISTRIBUTION OF SUITABLE HABITAT

Suitable prey densities for NARWs were found throughout the water column in the GSL during the summer season, with maximum densities found at 50 m in early summer (primarily sGSL) and at 230 m in late summer (primarily nGSL). NARWs have been observed foraging at various depths; from surface feeding often in late winter and spring, to feeding deeper in the water column during the summer and fall, and occasionally to the sea floor. Baumgartner and Mate (2003) and Baumgartner et al. (2017) found a positive correlation between NARW dive depth and the depth of maximum *C. finmarchicus* copepodite stage 5 (C5) abundance in the Gulf of Maine and southwestern Scotian Shelf during the summer, which often coincided with the depth of the bottom mixed layer. This boundary layer is created by tidal flow interacting with the bottom topography to generate a turbulent, well-mixed bottom layer. In the GSL, the water column during the summer is comprised of three distinct layers – the surface layer, the cold intermediate layer (CIL), and the deep-water layer. The CIL is formed by cool winter surface waters, which descend to depth during spring/summer, and is characterized by an average thickness of 20–100 m and temperature less than 1°C (Gilbert and Pettigrew 1997; Galbraith et al. 2017). Depths at which both diapausing *C. finmarchicus* and *C. hyperboreus* reach abundance maxima in the GSL are routinely below the lower boundary of the CIL (Krumhansl et al. 2018), the depth of which is influenced by local bathymetry (Melle et al. 2014). High abundance and occurrence probabilities of diapausing *Calanus* species have been associated with deep channels and basins in the GSL (Albouy-Boyer et al. 2016), such as the Laurentian Channel and Esquiman Channel. However, in the southern GSL, *Calanus* habitat selection for deeper depths when entering diapause is constrained by the shallow sea floor depth, which traps and concentrates *C. finmarchicus* and *C. hyperboreus* in shallower-than-normal waters during that stage, making them potentially more available to NARW in this area, which includes the Shediac Valley (Plourde et al. 2019). Diapausing *Calanus* occupy a broad range of temperatures, salinities, and densities (Sameoto and Herman 1990; Kaartvedt 1996; Heath et al. 2004; Krumhansl et al. 2018), however, where available, *Calanus* appear to favor depths with colder and denser waters, where temperatures less than 5°C are considered optimal for diapause (Saumweber and Durbin 2006). During spring and early summer, the depth of *C. finmarchicus* abundance maxima is likely variable, given they undertake diel vertical migrations. Increasing the temporal resolution of the depth-stratified zooplankton sampling design would allow better discrimination of depths likely targeted by NARW foraging in the GSL in early summer.

BIOENERGETICS

Our bioenergetics model evaluated how energy intake and expenditure varied with foraging depth within a modeled 3D prey field. We assumed energy gain was influenced by predator behaviour and morphology (daily time spent foraging, mouth gape), as well as prey nutritional value and density. Our resulting estimates of minimum prey densities required to satisfy daily energy expenditure (median 1.3 g m⁻³ resting; 1.8 g m⁻³ pregnant; 4.1 g m⁻³ lactating) agreed with minimum prey densities recorded in the vicinity of foraging NARWs on other feeding grounds (Table 7). Given that earlier studies often reported threshold prey densities as the number of copepods or zooplankton organisms m⁻³, we converted published values to g m⁻³ using a range of dry weights for *C. finmarchicus* stage-C5 and *C. hyperboreus* stage-C4 (0.0002–0.0006 g; Davies et al. 2012). Our minimum prey density estimates are closer to those measured *in situ* if one copepod weighs 0.0006g (Table 7). In future, it would be informative to compare the energetic value of *Calanus* species within the GSL (McKinstry et al. 2013), and when possible, collect prey species and density data near foraging NARWs.

Energy gain and thus prey density requirements also depend on time spent foraging daily and the number of days spent foraging per year. In this study, we used published values for daily foraging times, and modeled residency times on the breeding grounds in southeastern U.S. for female NARWs, and published estimates of migration duration to infer the number of days spent on feeding grounds. Compared to previous estimates of minimum residency times on the breeding grounds (Fortune et al. 2013), modeled mean residency times (Krzystan et al. 2018) were 1.7 times greater for non-calving females (23.6 d vs. 41.1 d) and 1.9 times greater for calving (lactating) females (46.3 d vs. 87.5 d). This leaves fewer days to be spent on feeding grounds for both classes, i.e., 17 d fewer days on feeding grounds for non-calving females, and 41 d fewer days for lactating females, if using modeled residency times. In turn, this would result in prey density requirements approximately 10% higher for resting and pregnant whales, and 20% higher for lactating females. If food stressed, females may choose to extend their stay on feeding grounds to search for food or forego migration to save energy. For part of the population, year-round foraging may occur, although food quality and availability likely varies throughout the year. There is evidence of a NARW giving birth in northeastern U.S. waters (Patrician et al. 2009), which may be an adaptive strategy to remain near food sources throughout the year. If this is the case, it will be of interest to monitor NARW occurrence, residency, and habitat use in northern latitudes such as the GSL during the winter period.

In this study, we assumed NARWs were physiologically capable of foraging at depths below maximum observed foraging depths (ca. 130–140 m; Nousek McGregor 2010; Baumgartner et al. 2017). The bowhead whale (*Balaena mysticetus*) shares similar morphological and ecological characteristics with right whales, and has been observed performing U-shaped dives (likely foraging) to a maximum depth of 427 m, and V-shaped dives (likely exploratory) to a maximum of 582 m (Heide-Jørgensen et al. 2013). Thus, we believe our assumption is plausible, although future NARW behavioural research could aim to document average and maximum depth of dives in the GSL, as well as how the water column is used throughout the season. This could inform the current model and support conservation efforts by assessing risk of ship strike and entanglement in various fishing gear and configurations (Baumgartner et al. 2017; Brillant et al. 2017).

As ocean temperatures continue to rise, *C. finmarchicus* are predicted to shift their distribution northward (Grieve et al. 2017). In the Gulf of Maine, sea surface temperature has increased at a rate three times faster than the global ocean average (Pershing et al. 2015; Saba et al. 2015). A consistent northward shift of *C. finmarchicus* has been observed in the North Atlantic, at a rate of around 8 km per decade (Chust et al. 2013), and multiple climate change models predict large declines of this key forage species in the western North Atlantic over the next three to four

decades (Reygondeau and Beaugrand 2010; Villarino et al. 2015; Grieve et al. 2017). Higher latitude feeding sites such as the GSL may become increasingly used by NARWs and other copepod predators.

REFERENCES CITED

- Albouy-Boyer, S., Plourde, S., Pepin, P., Johnson, C.L., Lehoux, C., Galbraith, P.S., Hebert, D., Lazin, G., and Lafleur, C. 2016. Habitat modelling of key copepod species in the Northwest Atlantic Ocean based on the Atlantic Zone Monitoring Program. *J. Plank. Res.* **38**(3): 589–603.
- Alexander, D.E. 1990. Drag coefficients of swimming animals: effects of using different reference areas. *Biol. Bull.* **179**(2): 186–190.
- Aoki, K., Watanabe, Y.Y., Crocker, D.E., Robinson, P.W., Biuw, M., Costa, D.P., Miyazaki, N., Fedak, M.A., and Miller, P.J.O. 2011. Northern elephant seals adjust gliding and stroking patterns with changes in buoyancy: validation of at-sea metrics of body density. *J. Exp. Biol.* **214**(17): 2973–2987. doi:10.1242/jeb.055137.
- Barrett, D.S., Triantafyllou, M.S., Yue, D.K.P., Grosenbaugh, M.A., and Wolfgang, M.J. 1999. [Drag reduction in fish-like locomotion](#). *J. Fluid Mech.* **392**: 183–212.
- Baumgartner, M., and Mate, B. 2003. Summertime foraging ecology of North Atlantic right whales. *Mar. Ecol. Prog. Ser.* **264**: 123–135.
- Baumgartner, M., Wenzel, F., Lysiak, N., and Patrician, M. 2017. North Atlantic right whale foraging ecology and its role in human-caused mortality. *Mar. Ecol. Prog. Ser.* **581**: 165–181.
- Beardsley, R.C., Epstein, A.W., Chen, C., Wishner, K.F., Macaulay, M.C., and Kenney, R.D. 1996. [Spatial variability in zooplankton abundance near feeding right whales in the Great South Channel](#). *Deep Sea Res. Part II Top. Stud. Oceanogr.* **43**(7): 1601–1625.
- Borazjani, I., and Sotiropoulos, F. 2008. Numerical investigation of the hydrodynamics of carangiform swimming in the transitional and inertial flow regimes. *J. Exp. Biol.* **211**(10): 1541–1558. doi:10.1242/jeb.015644.
- Brillant, S.W., Wimmer, T., Rangeley, R.W., and Taggart, C.T. 2017. [A timely opportunity to protect North Atlantic right whales in Canada](#). *Mar. Policy* **81**: 160–166.
- Brodie, P.F. 1975. Cetacean energetics, an overview of intraspecific size variation. *Ecology* **56**(1): 152–161.
- Brown, M.W., Fenton, D., Smedbol, K., Merriman, C., Robichaud-Leblanc, K., and Conway, J.D. 2009. Recovery Strategy for the North Atlantic Right Whale (*Eubalaena glacialis*) in Atlantic Canadian Waters [Final]. Species at Risk Act Recovery Strategy Series. Fisheries and Oceans Canada. : vi + 66p.
- Cameletti, M., Lindgren, F., Simpson, D., and Håvard, R. 2013. Spatio-temporal modeling of particulate matter concentration through the SPDE approach. *AStA Adv Stat Anal* **97**: 109–131.
- Chust, G., Castellani, C., Licandro, P., Ibaibarriaga, L., Sagarminaga, Y., and Irigoien, X. 2013. Are *Calanus* spp. shifting poleward in the North Atlantic? A habitat modelling approach. *ICES J. Mar. Sci.* **71**(2): 241–253.

-
- Cosandey-Godin, A., Krainski, E.T., Worm, B., and Flemming, J.M. 2014. [Applying Bayesian spatiotemporal models to fisheries bycatch in the Canadian Arctic](#). *Can. J. Fish. Aquat. Sci.* **72**(2): 186–197.
- Davies, K.T., Ryan, A., and Taggart, C.T. 2012. Measured and inferred gross energy content in diapausing *Calanus* spp. in a Scotian shelf basin. *J. Plank. Res.* **34**(7): 614–625.
- DFO. 2007. [Ecologically and Biologically Significant Areas \(EBSA\) in the Estuary and Gulf of St. Lawrence: identification and characterization](#). DFO Can. Sci. Advis. Secr. Sci. Advis. Rep. 2007/016.
- DFO. 2009. [Conservation objectives for the Ecologically and Biologically Significant Areas \(EBSA\) of the Estuary and Gulf of St. Lawrence](#). DFO Can. Sci. Advis. Secr. Sci. Advis. Rep. 2009/049.
- DFO. 2014. Recovery Strategy for the North Atlantic Right Whale (*Eubalaena glacialis*) in Atlantic Canadian Waters [Final]. Species at Risk Act Recovery Strategy Series. Fisheries and Oceans Canada, Ottawa. : vii + 68 pp.
- Dolphin, W.F. 1987. Ventilation and dive patterns of humpback whales, *Megaptera novaeangliae*, on their Alaskan feeding grounds. *Can. J. Zool.* **65**(1): 83–90. doi:10.1139/z87-013.
- Firestone, J., Lyons, S.B., Wang, C., and Corbett, J.J. 2008. Statistical modeling of North Atlantic right whale migration along the mid-Atlantic region of the eastern seaboard of the United States. *Biol. Conserv.* **141**(1): 221–232.
- Fish, F.E. 1993. Power output and propulsive efficiency of swimming bottlenose dolphins (*Tursiops truncatus*). *J. Exp. Biol.* **185**(1): 179–193.
- Fish, F. E. 1998. Comparative kinematics and hydrodynamics of odontocete cetaceans: morphological and ecological correlates with swimming performance. *J. Exp. Biol.* **201**(20): 2867-2877.
- Fish, F.E., and Rohr, J. 1999. Review of dolphin hydrodynamics and swimming performance. US Navy SPAWAR Syst. Cent. Tech. Rep. **1801**: 193 pp.
- Fish, F.E., Innes, S., and Ronald, K. 1988. Kinematics and estimated thrust production of swimming harp and ringed seals. *J. Exp. Biol.* **137**(1): 157–173.
- Fortune, S., Trites, A., Perryman, W., Moore, M., Pettis, H., and Lynn, M. 2012. Growth and rapid early development of North Atlantic right whales (*Eubalaena glacialis*). *J. Mammal.* **93**(5): 1342–1354.
- Fortune, S., Trites, A., Mayo, C., Rosen, D., and Hamilton, P. 2013. Energetic requirements of North Atlantic right whales and the implications for species recovery. *Mar. Ecol. Prog. Ser.* **478**: 253–272.
- Fuglstad, G.-A., Simpson, D., Lindgren, F., and Rue, H. 2018. Constructing priors that penalize the complexity of Gaussian Random Fields. *J. Am. Stat. Assoc.*: 1–8. doi:10.1080/01621459.2017.1415907.
- Galbraith, P.S., Chassé, J., Caverhill, C., Nicot, P., Gilbert, D., Pettigrew, B., Lefavre, D., Brickman, D., Devine, L., and Lafleur, C. 2017. [Physical oceanographic conditions in the Gulf of St. Lawrence in 2016](#). DFO Can. Sci. Advis. Secr. Res. Doc. 2017/044. v + 91 p.
- Gilbert, D., and Pettigrew, B. 1997. Interannual variability (1948-1994) of the CIL core temperature in the Gulf of St. Lawrence. *Can. J. Fish. Aquat. Sci.* **54**: 57–67.
-

-
- Gneiting, T., and Raftery, A.E. 2007. Strictly proper scoring rules, prediction, and estimation. *J. Am. Stat. Assoc.* **102**(477): 359–378. doi:10.1198/016214506000001437.
- Goodyear, J.D. 1996. Significance of feeding habitats of North Atlantic right whales based on studies of diel behaviour, diving, food ingestion rates, and prey. PhD thesis. Guelph University.
- Grieve, B.D., Hare, J.A., and Saba, V.S. 2017. Projecting the effects of climate change on *Calanus finmarchicus* distribution within the U.S. Northeast Continental Shelf. *Sci. Rep.* **7**(1): 6264. doi:10.1038/s41598-017-06524-1.
- Hall, C.A.S., Stanford, J.A., and Hauer, F.R. 1992. The distribution and abundance of organisms as a consequence of energy balances along multiple environmental gradients. *Oikos* **65**(3): 377–390. doi:10.2307/3545553.
- Hamilton, P.K., and Cooper, L.A. 2010. Changes in North Atlantic right whale (*Eubalaena glacialis*) cow–calf association times and use of the calving ground: 1993–2005. *Mar. Mammal Sci.* **26**(4): 896–916. doi:10.1111/j.1748-7692.2010.00378.x.
- Hamilton, P.K., Marx, M.K., and Kraus, S.D. 1995. Weaning in North Atlantic right whales. *Mar. Mammal Sci.* **11**(3): 386–390.
- Hays, G., Marshall, G., and Seminoff, J. 2007. [Flipper beat frequency and amplitude changes in diving green turtles, *Chelonia mydas*](#). *Mar. Biol.* **150**(5): 1003–1009.
- Heath, M.R., Boyle, P.R., Gislason, A., Gurney, W.S.C., Hay, S.J., Head, E.J.H., Holmes, S., Ingvarsdóttir, A., Jónasdóttir, S.H., Lindeque, P., Pollard, R.T., Rasmussen, J., Richards, K., Richardson, K., Smerdon, G., and Speirs, D. 2004. Comparative ecology of over-wintering *Calanus finmarchicus* in the northern North Atlantic, and implications for life-cycle patterns. *ICES J. Mar. Sci.* **61**(4): 698–708.
- Heide-Jørgensen, M.P., Laidre, K.L., Nielsen, N.H., Hansen, R.G., and Røstad, A. 2013. [Winter and spring diving behavior of bowhead whales relative to prey](#). *Anim. Biotelemetry* **1**(1): 15.
- Hertel, H. 1969. Hydrodynamics of swimming and wave-riding dolphins. *In* *The Biology of Marine Mammals*. Edited by H.T. Andersen. Academic Press, New York, USA. pp. 31–63.
- Hind, A.T., and Gurney, W.S. 1997. The metabolic cost of swimming in marine homeotherms. *J. Exp. Biol.* **200**(3): 531–542.
- Kaartvedt, S. 1996. [Habitat preference during overwintering and timing of seasonal vertical migration of *Calanus finmarchicus*](#). *Ophelia* **44**(1–3): 145–156.
- Kaye, G.W.C., and Laby, T.H. 1995. Tables of Physical and Chemical Constants (16th edition 1995). 2.1.4 Hygrometry. Kaye and Laby Online. Version 1.0 (2005).
- Kenney, R. D., Hyman, M. A., Owen, R. E., Scott, G. P., and Winn, H. E. 1986. Estimation of prey densities required by western North Atlantic right whales. *Mar. Mamm. Sci.* **2**(1), 1-13.
- Kleiber, M. 1961. *The fire of life. An introduction to animal energetics*. Krieger Pub Co., New York, USA.
- Kleiber, M. 1975. [Metabolic turnover rate: A physiological meaning of the metabolic rate per unit body weight](#). *J. Theor. Biol.* **53**(1): 199–204.
- Kline, S.J., Reynolds, W.C., Schraub, F.A., and Runstadler, P.W. 1967. The structure of turbulent boundary layers. *J. Fluid Mech.* **30**(4): 741–773.
- Knowlton, A.R., Kraus, S.D., and Kenney, R.D. 1994. [Reproduction in North Atlantic right whales \(*Eubalaena glacialis*\)](#). *Can. J. Zool.* **72**(7): 1297–1305.
-

-
- Krainski, E.T., Lindgren, F., Simpson, D., and Havard, R. 2017. [The R-INLA tutorial on SPDE models](#).
- Kraus, S., and Prescott, J. 1982. The North Atlantic right whale (*Eubalaena glacialis*) in the Bay of Fundy, 1981, with notes on the distribution, abundance, biology and behavior. Final report to the U.S. Department of Commerce, National Marine Fisheries Service, and World Wildlife-US.
- Kraus, S., Kenney, R., Mayo, C., McLellan, W., Moore, M., and Nowacek, D. 2016. Recent scientific publications cast doubt on North Atlantic right whale future. *Front. Mar. Sci.* **3**: 137.
- Krumhansl, K.A., Head, E.J.H., Pepin, P., Plourde, S., Record, N.R., Runge, J.A., and Johnson, C.L. 2018. [Environmental drivers of vertical distribution in diapausing *Calanus* copepods in the Northwest Atlantic](#). *Prog. Oceanogr.* **162**: 202–222.
- Krzystan, A.M., Gowan, T.A., Kendall, W.L., Martin, J., Ortega-Ortiz, J.G., Jackson, K., Knowlton, A.R., Naessig, P., Zani, M., Schulte, D.W., and Taylor, C.R. 2018. Characterizing residence patterns of North Atlantic right whales in the southeastern USA with a multistate open robust design model. *Endanger. Species Res.* **36**: 279–295.
- Lavoie, D., Starr, M., Zakardjian, B., and Larouche, P. 2007. [Identification of ecologically and biologically significant areas \(EBSA\) in the Estuary and Gulf of St. Lawrence: Primary production](#). DFO Can. Sci. Advis. Sec. Sci. Advis. Rep. 2007/079.
- Lehoux, C., Plourde S., and Lesage, V. 2020. Significance of dominant zooplankton species to the North Atlantic Right Whale potential foraging habitats in the Gulf of St. Lawrence: a bio-energetic approach. DFO Can. Sci. Advis. Sec. Res. Doc. 2020/033. iv + 44 p.
- Lindgren, F., Håvard, R., and Lindström, J. 2011. [An explicit link between Gaussian fields and Gaussian Markov random fields: the stochastic partial differential equation approach](#). *J. R. Stat. Soc. B* **73**(4): 423–49.
- Lockyer, C. 1981. Estimation of the energy costs of growth, maintenance and reproduction in the female minke whale, (*Balaenoptera acutorostrata*), from the southern hemisphere. *Reports Int. Whal. Comm.* **31**: 337–343.
- Lockyer, C. 1984. Review of baleen whale (Mysticeti) reproduction and implications for management. *Reports Int. Whal. Comm.* **6**: 27–50.
- Lockyer, C. 2007. All creatures great and smaller: a study in cetacean life history energetics. *J. Mar. Biol. Assoc. United Kingdom* **87**(4): 1035–1045.
- Maps, F., Plourde, S., McQuinn, I.H., St-Onge-Drouin, S., Lavoie, D., Chassé, J., and Lesage, V. 2015. [Linking acoustics and finite-time Lyapunov exponents reveals areas and mechanisms of krill aggregation within the Gulf of St. Lawrence, eastern Canada](#). *Limnol. Oceanogr.* **60**(6): 1965–1975. Wiley-Blackwell.
- Mayo, C.A., and Goldman, L. 1992. Right whale foraging and the plankton resources in Cape Cod and Massachusetts Bays. *In* The right whale in the western North Atlantic: a science and management workshop. *Edited by* J. Hain. pp. 43–44.
- Mayo, C.A., and Marx, M.K. 1990. [Surface foraging behaviour of the North Atlantic right whale, *Eubalaena glacialis*, and associated zooplankton characteristics](#). *Can. J. Zool.* **68**(10): 2214–2220. NRC Research Press.
- Mayo, C.A., Letcher, B.H., and Scott, S. 2001. Zooplankton filtering efficiency of the baleen of a North Atlantic right whale, *Eubalaena glacialis*. *J. Cetacean Res. Manag.* **3**: 245–250.
-

-
- McKinstry, C., Westgate, A., and Koopman, H. 2013. Annual variation in the nutritional value of Stage V *Calanus finmarchicus*: implications for right whales and other copepod predators. *Endanger. Species Res.* **20**(3): 195–204.
- McNab, B.K. 2002. *The physiological ecology of vertebrates: a view from energetics*. Cornell University Press.
- Melle, W., Runge, J., Head, E., Plourde, S., Castellani, C., Licandro, P., Pierson, J., Jonasdottir, S., Johnson, C., Broms, C., Debes, H., Falkenhaus, T., Gaard, E., Gislason, A., Heath, M., Niehoff, B., Nielsen, T.G., Pepin, P., Stenevik, E.K., and Chust, G. 2014. [The North Atlantic Ocean as habitat for *Calanus finmarchicus*: Environmental factors and life history traits](#). *Prog. Oceanogr.* **129**: 244–284.
- Michaud, J., and Taggart, C.T. 2011. Spatial variation in right whale food, *Calanus finmarchicus*, in the Bay of Fundy. *Endang Species Res* **15**: 179-194.
- Miller, C., Best, P., Perryman, W., Baumgartner, M., and Moore, M. 2012a. Body shape changes associated with reproductive status, nutritive condition and growth in right whales *Eubalaena glacialis* and *E. australis*. *Mar. Ecol. Prog. Ser.* **459**: 135–156.
- Miller, P.J.O., Johnson, M., Tyack, P., and Terray, E. 2004. Swimming gaits, passive drag and buoyancy of diving sperm whales *Physeter macrocephalus*. *J. Exp. Biol.* **207**(11): 1953–1967. doi: 10.1242/jeb.00993.
- Miller, P.J.O., Biuw, M., Watanabe, Y.Y., Thompson, D., and Fedak, M.A. 2012b. Sink fast and swim harder! Round-trip cost-of-transport for buoyant divers. *J. Exp. Biol.* **215**(20): 3622–3630. doi:10.1242/jeb.070128.
- Miller, P., Narazaki, T., Isojunno, S., Aoki, K., Smout, S., and Sato, K. 2016. Body density and diving gas volume of the northern bottlenose whale (*Hyperoodon ampullatus*). *J. Exp. Biol.* **219**(16): 2458–2468.
- Moore, M., Knowlton, A., Kraus, S., McLellan, W., and Bonde, R. 2005. Morphometry, gross morphology and available histopathology in North Atlantic right whale (*Eubalaena glacialis*) mortalities (1970 to 2002). *J. Cetacean Res. Manag.* **6**(3): 199–214.
- Murison, L.D., and Gaskin, D.E. 1989. [The distribution of right whales and zooplankton in the Bay of Fundy, Canada](#). *Can. J. Zool.* **67**(6): 1411–1420.
- Nelson, T., Duffus, D., Robertson, C., Laberee, K., and Feyrer, L. 2009. Spatial-temporal analysis of marine wildlife. *J. Coast. Res.*: 1537–1541.
- New, L.F., Moretti, D.J., Hooker, S.K., Costa, D.P., and Simmons, S.E. 2013. [Using energetic models to investigate the survival and reproduction of Beaked Whales \(family Ziphiidae\)](#). *PLoS One* **8**(7).
- Nikolioudakis, N., Skaug, H., Olafsdottir, A., Jansen, T., Jacobsen, J., and Enberg, K. 2018. Drivers of the summer-distribution of Northeast Atlantic mackerel (*Scomber scombrus*) in the Nordic Seas from 2011 to 2017; a Bayesian hierarchical modelling approach. *ICES J. Mar. Sci.*: 1–19.
- Nousek McGregor, A.E. 2010. *The cost of locomotion in North Atlantic right whales *Eubalaena glacialis**. PhD thesis. Duke University.
- Nousek-McGregor, A.E., Miller, C.A., Moore, M.J., and Nowacek, D.P. 2014. [Effects of body condition on buoyancy in endangered North Atlantic right whales](#). *Physiol. Biochem. Zool.* **87**(1): 160–171.
-

-
- Nowacek, D.P., Johnson, M.P., Tyack, P.L., Shorter, K.A., McLellan, W.A., and Pabst, D.A. 2001. Buoyant balaenids: the ups and downs of buoyancy in right whales. Proc. R. Soc. London. Ser. B Biol. Sci. **268**(1478): 1811–1816.
- Oftedal, O.T. 1997. [Lactation in whales and dolphins: evidence of divergence between baleen- and toothed-species](#). J. Mammary Gland Biol. Neoplasia **2**(3): 205–230.
- Olsson, O., and Bolin, A. 2014. [A model for habitat selection and species distribution derived from central place foraging theory](#). Oecologia **175**(2): 537–548.
- Pace, R.M., Corkeron, P.J., and Kraus, S.D. 2017. [State–space mark–recapture estimates reveal a recent decline in abundance of North Atlantic right whales](#). Ecol. Evol. **7**(21): 8730–8741.
- Parks, S., Searby, A., Célérier, A., Johnson, M., Nowacek, D., and Tyack, P. 2011. Sound production behavior of individual North Atlantic right whales: implications for passive acoustic monitoring. Endanger. Species Res. **15**(1): 63–76.
- Patrician, M.R., Biedron, I.S., Esch, H.C., Wenzel, F.W., Cooper, L.A., Hamilton, P.K., Glass, A.H., and Baumgartner, M.F. 2009. Evidence of a North Atlantic right whale calf (*Eubalaena glacialis*) born in northeastern U.S. waters. Mar. Mammal Sci. **25**(2): 462–477. doi:10.1111/j.1748-7692.2008.00261.x.
- Pershing, A.J., Alexander, M.A., Hernandez, C.M., Kerr, L.A., Le Bris, A., Mills, K.E., Nye, J.A., Record, N.R., Scannell, H.A., Scott, J.D., Sherwood, G.D., and Thomas, A. 2015. Slow adaptation in the face of rapid warming leads to collapse of the Gulf of Maine cod fishery. Science. **350**(6262): 809–812.
- Peterson, A., Papeş, M., and Soberón, J. 2015. [Mechanistic and correlative models of ecological niches](#). Eur. J. Ecol. **1**(2): 28–38.
- Pettis, H., and Hamilton, P. 2016. North Atlantic Right Whale Consortium 2016 Annual Report Card. Report to the North Atlantic Right Whale Consortium.
- Pettis, H., Pace, R.M., Schick, R.S., and Hamilton, P.K. 2018. North Atlantic Right Whale Consortium 2017 Annual Report Card. Report to the North Atlantic Right Whale Consortium.
- Phillips, A.B., Haroutunian, M., Murphy, A.J., Boyd, S.W., Blake, J.I.R., and Griffiths, G. 2017. [Understanding the power requirements of autonomous underwater systems, Part I: An analytical model for optimum swimming speeds and cost of transport](#). Ocean Eng. **133**: 271–279.
- Plourde, S., Lehoux, C., McQuinn, I.H., and Lesage, V. 2016. [Describing krill distribution in the western North Atlantic using statistical habitat models](#). DFO Can. Sci. Advis. Secr. Res. Doc. 2016/111: v + 34 p.
- Plourde, S., Lehoux, C., Johnson, C.L., Perrin, G., and Lesage, V. 2019. [North Atlantic right whale \(*Eubalaena glacialis*\) and its food: \(I\) a spatial climatology of *Calanus* biomass and potential foraging habitats in Canadian waters](#). J. Plank. Res. **41**(5) 667-685.
- Potvin, J., and Werth, A.J. 2017. Oral cavity hydrodynamics and drag production in Balaenid whale suspension feeding. PLoS One **12**(4): e0175220.
- Rechsteiner, E.U., Rosen, D.A.S., and Trites, A.W. 2013. [Energy requirements of Pacific white-sided dolphins \(*Lagenorhynchus obliquidens*\) as predicted by a bioenergetic model](#). J. Mammal. **94**(4): 820–832.
- Reygondeau, G., and Beaugrand, G. 2010. [Future climate-driven shifts in distribution of *Calanus finmarchicus*](#). Glob. Chang. Biol. **17**(2): 756–766.
-

-
- Reynolds, O. 1883. XXIX. An experimental investigation of the circumstances which determine whether the motion of water shall be direct or sinuous, and of the law of resistance in parallel channels. *Philos. Trans. R. Soc. London* **174**: 935–982.
- Saba, V.S., Griffies, S.M., Anderson, W.G., Winton, M., Alexander, M.A., Delworth, T.L., Hare, J.A., Harrison, M.J., Rosati, A., Vecchi, G.A., and Zhang, R. 2015. [Enhanced warming of the Northwest Atlantic Ocean under climate change](#). *J. Geophys. Res. Ocean.* **121**(1): 118–132.
- Sameoto, D.D., and Herman, A.W. 1990. Life cycles and distribution of *Calanus finmarchicus* in deep basins on the Nova Scotia shelf and seasonal changes in *Calanus* spp. *Mar. Ecol. Prog. Ser.* **66**: 225–237.
- Sanderson, S.L., and Wassersug, R. 1990. Suspension-feeding vertebrates. *Sci. Am.* **262**(3): 96–102.
- Sato, K., Shiomi, K., Watanabe, Y., Watanuki, Y., Takahashi, A., and Ponganis, P.J. 2010. Scaling of swim speed and stroke frequency in geometrically similar penguins: they swim optimally to minimize cost of transport. *Proc. R. Soc. B Biol. Sci.* **277**(1682): 707–714.
- Saumweber, W.J., and Durbin, E.G. 2006. [Estimating potential diapause duration in *Calanus finmarchicus*](#). *Deep Sea Res. Part II Top. Stud. Oceanogr.* **53**(23): 2597–2617.
- Schmidt-Nielsen, K. 1997. *Animal Physiology: Adaptation and Environment*, 5th edn. Cambridge University Press, Cambridge.
- Sibly, R.M., and Calow, P. 1986. *Physiological ecology of animals*. Blackwell Scientific Publications, Oxford.
- Sibly, R.M., Grimm, V., Martin, B.T., Johnston, A.S.A., Kułakowska, K., Topping, C.J., Calow, P., Nabe-Nielsen, J., Thorbek, P., and DeAngelis, D.L. 2012. [Representing the acquisition and use of energy by individuals in agent-based models of animal populations](#). *Methods Ecol. Evol.* **4**(2): 151–161.
- Simpson, D., Rue, H., Riebler, A., Martins, T.G., and Sørbye, S.H. 2017. Penalising model component complexity: A principled, practical approach to constructing priors. *Stat. Sci.* **32**: 1–28.
- Slijper, E.J. 1966. Functional morphology of the reproductive system in Cetacea. *In Whales, dolphins, and porpoises. Edited by K.S. Norris*. University of California Press. pp. 277–319.
- Sorochan, K. A., Plourde, S., Morse, R., Pepin, P., Runge, J., Thompson, C., and Johnson, C. L. 2019. North Atlantic right whale (*Eubalaena glacialis*) and its food: (II) interannual variations in biomass of *Calanus* spp. on northwest Atlantic shelves. *J. Plank. Res.*, 41(5), 687-708.
- Spiegelhalter, D.J., Best, N.G., Carlin, B.P., and van der Linde, A. 2002. Bayesian measures of model complexity and fit. *J. R. Stat. Soc. Ser. B* **64**(4): 583–639.
- Stephens, D.W., and Krebs, J.R. 1986. [Foraging theory](#). Princeton University Press, Princeton, New Jersey.
- Swaim, Z., Westgate, A., Koopman, H., Rolland, R., and SD, K. 2009. [Metabolism of ingested lipids by North Atlantic right whales](#). *Endanger. Species Res.* **6**(3): 259–271.
- Thompson, D., and Fedak, M.A. 2001. [How long should a dive last? A simple model of foraging decisions by breath-hold divers in a patchy environment](#). *Anim. Behav.* **61**(2): 287–296.
- Tomilin, A. 1967. *Mammals of the USSR and adjacent countries*. Vol. 9, Cetacea. Israel Program for Scientific Translations (translator), Jerusalem.
-

-
- Trassinelli, M. 2016. Energy cost and optimisation in breath-hold diving. *J. Theor. Biol.* **396**: 42–52. doi: 10.1016/j.jtbi.2016.02.009.
- Tucker, V. 1975. The energetic cost of moving about: walking and running are extremely inefficient forms of locomotion. Much greater efficiency is achieved by birds, fish-and bicyclists. *Am. Sci.* **63**(4): 413–419.
- van der Hoop, J., Moore, M., Fahlman, A., Bocconcelli, A., George, C., Jackson, K., Miller, C., Morin, D., Pitchford, T., Rowles, T., Smith, J., and Zoodsma, B. 2013. [Behavioral impacts of disentanglement of a right whale under sedation and the energetic cost of entanglement](#). *Mar. Mammal Sci.* **30**(1): 282–307.
- van der Hoop, J., Corkeron, P., and Moore, M. 2016. [Entanglement is a costly life-history stage in large whales](#). *Ecol. Evol.* **7**(1): 92–106.
- van der Hoop, J.M. Nowacek, D.P., Moore, M.J., and Triantafyllou, M.S. 2017. Swimming kinematics and efficiency of entangled North Atlantic right whales. *Endanger. Species Res.* **32**: 1–17.
- van der Hoop, J.M., Nousek-McGregor, A.E., Nowacek, D.P., Parks, S.E., Tyack, P., and Madsen, P.T. 2019. [Foraging rate of ram-filtering North Atlantic right whales](#). *Funct. Ecol.*
- Vermeulen, E., Cammareri, A., and Holsbeek, L. 2012. Alteration of southern right whale (*Eubalaena australis*) behaviour by human-induced disturbance in Bahía San Antonio, Patagonia, Argentina. *Aquat. Mamm.* **38**(1): 56–64.
- Villarino, E., Chust, G., Licandro, P., Butenschön, M., Ibaibarriaga, L., Larrañaga, A., and Irigoien, X. 2015. Modelling the future biogeography of North Atlantic zooplankton communities in response to climate change. *Mar. Ecol. Prog. Ser.* **531**: 121–142.
- Villegas-Amtmann, S., Schwarz, L.K., Sumich, J.L., and Costa, D.P. 2015. [A bioenergetics model to evaluate demographic consequences of disturbance in marine mammals applied to gray whales](#). *Ecosphere* **6**(10): 1–19.
- Vogel, S. 1994. *Life in Moving Fluids; The Physical Biology of Flow*, 2nd ed. Princeton University Press, Princeton, New Jersey.
- von Kármán, T., and Millikan, C.B. 1934. On the theory of laminar boundary layers involving separation. National Advisory Committee on Aeronautics, Washington, DC. **504**: 541–560.
- Watanabe, S. 2010. Asymptotic equivalence of Bayes cross validation and widely applicable information criterion in singular learning theory. *J. Mach. Learn. Res.* **11**(Dec): 3571–3594.
- Watkins, W.A., and Schevill, W.E. 1976. Right whale feeding and baleen rattle. *J. Mammal.* **57**(1): 58–66.
- Webb, P. 1975. Hydrodynamics and energetics of fish propulsion. *Bull. Fish. Res. Board Canada* **190**: 1–159.
- Williams, T.M., and Kooyman, G.L. 1985. [Swimming performance and hydrodynamic characteristics of harbor seals *Phoca vitulina*](#). *Physiol. Zool.* **58**(5): 576–589.
- Williams, T., and Maresh, J. 2015. Exercise energetics. *In Marine Mammal Physiology: Requisites for Ocean Living. Edited by M.A. Castellini and J.-A. Mellish.* CRC Press Taylor & Francis Group, Boca Raton, FL. pp. 47–68.
- Williams, T., Davis, R., Fuiman, L., Francis, J., Le Boeuf, B.J., Horning, M., Calambokidis, J., and Croll, D. 2000. Sink or swim: strategies for cost-efficient diving by marine mammals. *Science.* **288**(5463): 133–136.
-

-
- Winn, H., Price, C., and Sorensen, P. 1986. The distributional biology of the right whale (*Eubalaena glacialis*) in the western North Atlantic. Reports Int. Whal. Comm. Spec. Issue 10: 129–138.
- Wishner, K.F., Schoenherr, J.R., Beardsley, R., and Chen, C. 1995. [Abundance, distribution and population structure of the copepod *Calanus finmarchicus* in a springtime right whale feeding area in the southwestern Gulf of Maine](#). Cont. Shelf Res. **15**(4): 475–507.
- Woodward, B.L., Winn, J.P., and Fish, F.E. 2006. [Morphological specializations of baleen whales associated with hydrodynamic performance and ecological niche](#). J. Morphol. **267**(11): 1284–1294.

TABLES

Table 1. List of parameters used in bioenergetic model.

Symbol	Parameter (unit)	Value	Reference
α	Skin friction coefficient constant	0.072	See Methods
A	Total wetted surface area (m ²)	0.08mass ^{0.65}	Alexander (1990); Fish (1993)
A_m	Mouth opening area (m ²)	1.7, 1.9	van der Hoop et al. (2019)
β	Skin friction coefficient exponent	-0.2	See Methods
d	Body diameter (m)	3.15	Nousek McGregor (2010)
D_p	Prey density (g m ⁻³)		This study
E_p	Prey energy content (MJ g ⁻¹)	0.0229, 0.0329	Davies et al. (2012)
ϵ_A	Dietary assimilation efficiency	0.80, 0.92	Lockyer (1981); Swaim et al. (2009)
g	Appendage drag	1.3	Fish and Rohr (1999); van der Hoop (2013)
L	Adult NARW body length (m)	14	Moore et al. (2005)
mass	Adult NARW body mass (kg)	35000	Moore et al. (2005)
mass _{nb}	Newborn NARW body mass (kg)	790, 1412	Fortune et al. (2012)
η_m	Muscular/metabolic efficiency	0.25	Kleiber (1961); Webb (1975)
η_p	Propulsive/propeller efficiency	0.51	van der Hoop et al. (2017)
t_b	Bottom time (time spent ingesting prey; s)	≤150 m: 0.0704·depth > 150 m: 636	Baumgartner et al. (2017) See Methods
t_s	Post-dive surface time (s)	Resting: 0.211·total time at depth; Pregnant/Lactating: 0.342·total time at depth	Baumgartner and Mate (2003)
t_{glide}	Proportion of time spent gliding	Surface/travel: 0.09 Ascent: 0.30; Descent: 0.36 Bottom/foraging: 0.09	Nowacek et al. (2001); Nousek McGregor (2010); Nousek McGregor et al. (2014)
U_b	Foraging swim speed (m s ⁻¹)	1.0	Baumgartner and Mate (2003); Nousek McGregor (2010)
U_a, U_d	Ascent, descent swim speed (m s ⁻¹)	1.45	Baumgartner et al. (2017)
U_t	Travel speed (m s ⁻¹)	2.0	Tomilin (1967) as cited in Woodward et al. (2006); Goodyear (1996)
ν	Kinematic viscosity of seawater (m ² s ⁻¹)	1.83 x 10 ⁻⁶	Kaye and Laby (1995)
γ	Surface wave drag	1.0	See Methods
ρ	Density of seawater (kg m ⁻³)	1028	Miller et al. (2016)
λ	Active-to-passive drag ratio	1.0	See Methods
θ	Body angle during dive (°)	Ascent: 62 Descent: 74	Nousek-McGregor et al. (2014)

Table 2. Inferred daily and seasonal time-activity budget for North Atlantic right whale adult females. Note annual phase durations are identical for resting and pregnant females. Travelling and socializing behavior are grouped together for energy expenditure calculation.

Annual phase	Phase duration per reproductive stage (days year ⁻¹)			Foraging time (h day ⁻¹)	Travelling time (h day ⁻¹)	Resting time (h day ⁻¹)
	Resting	Pregnant	Lactating			
Summer foraging	261.5–296.9	261.5–296.9	217.4–244.1	15.1 ⁴ –17.2 ⁵	6.2 ⁵ –8.3 ⁴	0.6 ^{4,5}
Fall migration		21–24 ¹		0	20 ¹	4 ⁶
Winter breeding	26.1–55.5 ²	26.1–55.5 ²	78.9–99.6 ²	0	19.9–21.4 ³	2.6–4.1 ³
Spring migration		21–24 ¹		0	20 ¹	4 ⁶

¹ Firestone et al. (2008): Average travel time of 21–24 days departure from Jacksonville, Florida to the tip of Long Island (ca. 1500km); migration distance to GSL approx. 2775 km from Jacksonville; here, we assume NARW begin to forage after 21-24 d migration

² Krzystan et al. (2018): Modeled residency times on winter breeding grounds for non-calving (resting, pregnant) and calving (lactating) female NARWs

³ Vermeulen et al. (2012): Inferred from Southern right whale (*Eubalaena australis*) activity budget on breeding ground. Travel (41%) and social (42%) activity grouped together and resting (11%) and ‘other’ (6%) activity grouped together. Nousek McGregor (2010) found tagged right whales on breeding ground off Florida, USA to spend 64.7% of their time (174/269 dives) presumably travelling (deeper and longer dives) and 35.3% (95/269) of their time either socializing or resting (shallower and shorter dives).

⁴ Goodyear (1996): Estimated mean daily activity budget from NARW tag data in the Bay of Fundy as: Foraging (62.8%; 15.07h per day), Socializing: (18.15%), Traveling (15.8%), Resting (2.7%; 0.65h per day), Playing (0.6%). For this model, we combined social, travel and play activity together: 34.9% (or 8.38h per day)

⁵ Parks et al. (2011): Estimated mean daily activity budget from NARW tag data in the Bay of Fundy as: Foraging (71.7%; 17.2h per day), Socializing: (4.7%), Traveling (21.3%), Resting (2.37%; 0.57h per day). For this model, we combined social and travel activity together: 26% (or 6.24h per day)

⁶ Assumption

Table 3. Methods summarized in five steps.

Step	Description	Approach
1	Render point sampling observations of <i>Calanus</i> biomass into a 2D continuous prey field, accounting for spatial autocorrelation	Bayesian hierarchical spatial model
2	Project continuous prey field onto a regular 10km ² grid covering study area	Bayesian hierarchical spatial model
3	Apply <i>Calanus</i> vertical distribution model to transform prey field from 2D to 3D	Generalized additive model
4	Apply right whale foraging bioenergetics model to transform 3D prey field into a 3D net energy field	Theoretical time-energy budget bioenergetics model
5	Convert net energy field into a foraging habitat suitability grid	Summarize relative foraging value of each grid cell across space (study area) and time (12-year study period)

Table 4. Depth-integrated *Calanus* spp. biomass sample sizes (number of stations sampled) from 2006 to 2017, for early summer (June–early July) and late summer (late July–September) periods.

	2006	2007	2008	2009	2010	2011	2012	2013	2014	2015	2016	2017
Early summer	64	67	51	60	65	66	66	65	67	59	65	65
Late summer	90	98	80	89	74	77	82	56	76	35	NA	26
Total	154	165	131	149	139	143	148	121	143	94	65	91

Table 5. Summary of depth-integrated *Calanus* biomass (g dry weight m⁻²) predictions for early and late season, 2006–2017 at 10km² grid locations in the Gulf of St. Lawrence.

Year	Summer season	Median	Mean	SD	Min	Max
2006	Early	46.97	56.73	71.18	0.74	506.40
2007	Early	56.66	71.61	61.26	2.79	477.39
2008	Early	39.72	43.40	36.95	4.26	458.76
2009	Early	34.26	42.36	47.13	6.80	451.89
2010	Early	3.09	30.17	83.25	0.97	492.01
2011	Early	20.38	48.52	79.96	0.19	490.40
2012	Early	41.72	51.29	44.90	13.69	463.68
2013	Early	29.00	48.28	68.51	11.70	505.63
2014	Early	10.34	36.43	57.16	0.10	472.64
2015	Early	0.68	2.62	6.74	0.06	95.55
2016	Early	2.81	19.02	58.57	0.00	478.86
2017	Early	6.72	19.84	46.48	0.25	456.89
2006	Late	7.70	22.33	25.35	0.64	102.60
2007	Late	14.57	34.62	35.88	4.25	126.41
2008	Late	12.49	43.72	53.99	1.15	242.85
2009	Late	12.68	37.39	50.88	0.49	372.98
2010	Late	2.09	13.80	21.09	0.64	94.46
2011	Late	2.01	15.98	22.67	0.18	117.82
2012	Late	3.09	18.39	23.32	0.85	113.06
2013	Late	12.63	32.52	31.33	4.96	126.86
2014	Late	14.69	25.72	23.98	1.06	120.04
2015	Late	27.43	39.57	36.43	5.00	404.78
2017	Late	9.52	15.79	11.26	3.95	41.87

Table 6. Estimated daily energy expenditure (MJ day^{-1}) for a 14-m adult female North Atlantic right whale in either a resting, pregnant or lactating reproductive state.

Reproductive state	Min.	Median	Max.
Resting	1355	1533	1726
Pregnant	1557	1855	2167
Lactating	3565	4233	4915

Table 7. Minimum prey density thresholds measured around foraging North Atlantic right whales. Density threshold in g m^{-3} calculated based on an individual copepod dry weight of either 0.0002g or 0.0006g (Davies et al. 2012). BoF: Bay of Fundy, CCB: Cape Cod Bay, GoM: Gulf of Maine, RB: Roseway Basin.

Reference	Location	Density threshold (copepods or organisms m^{-3})	Density threshold (g m^{-3})	Individual copepod weight (g)
Murison and Gaskin (1989)	BoF	820 cope.	0.2	0.0002
			0.5	0.0006
Mayo and Marx (1990)	CCB	1000 org.	0.2	0.0002
			0.6	0.0006
Mayo and Goldman (1992)	GoM	4000 cope.	0.8	0.0002
			2.4	0.0006
Wishner et al. (1995)	GoM	1023–9749 cope.	0.2–2.0	0.0002
			0.6–5.8	0.0006
Beardsley et al. (1996)	GoM	1500–4500 cope.	0.3–0.9	0.0002
			1.0–3.0	0.0006
Baumgartner and Mate (2003)	BoF and RB	3000 cope.	0.6	0.0002
			1.8	0.0006

FIGURES

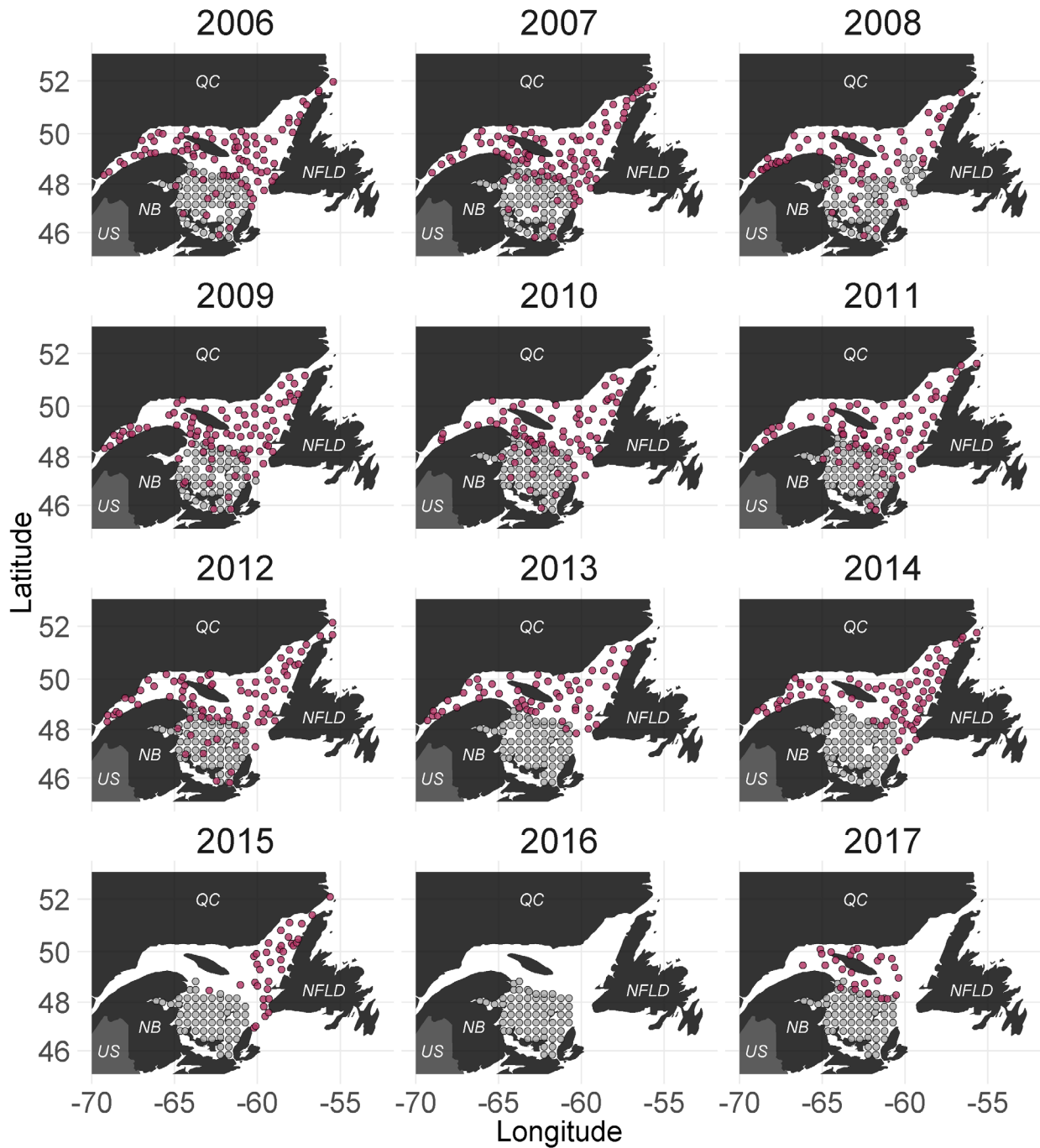


Figure 1. *Calanus copepod* sampling locations in the Estuary and Gulf of St. Lawrence, Canada from 2006 to 2017. Early summer season sampling (June-early July) occurred in the southern Gulf of St. Lawrence (grey points) and late summer season sampling (late July-September) occurred primarily in the northern Gulf of St. Lawrence (maroon points). Note that in 2016, only early season data was available.

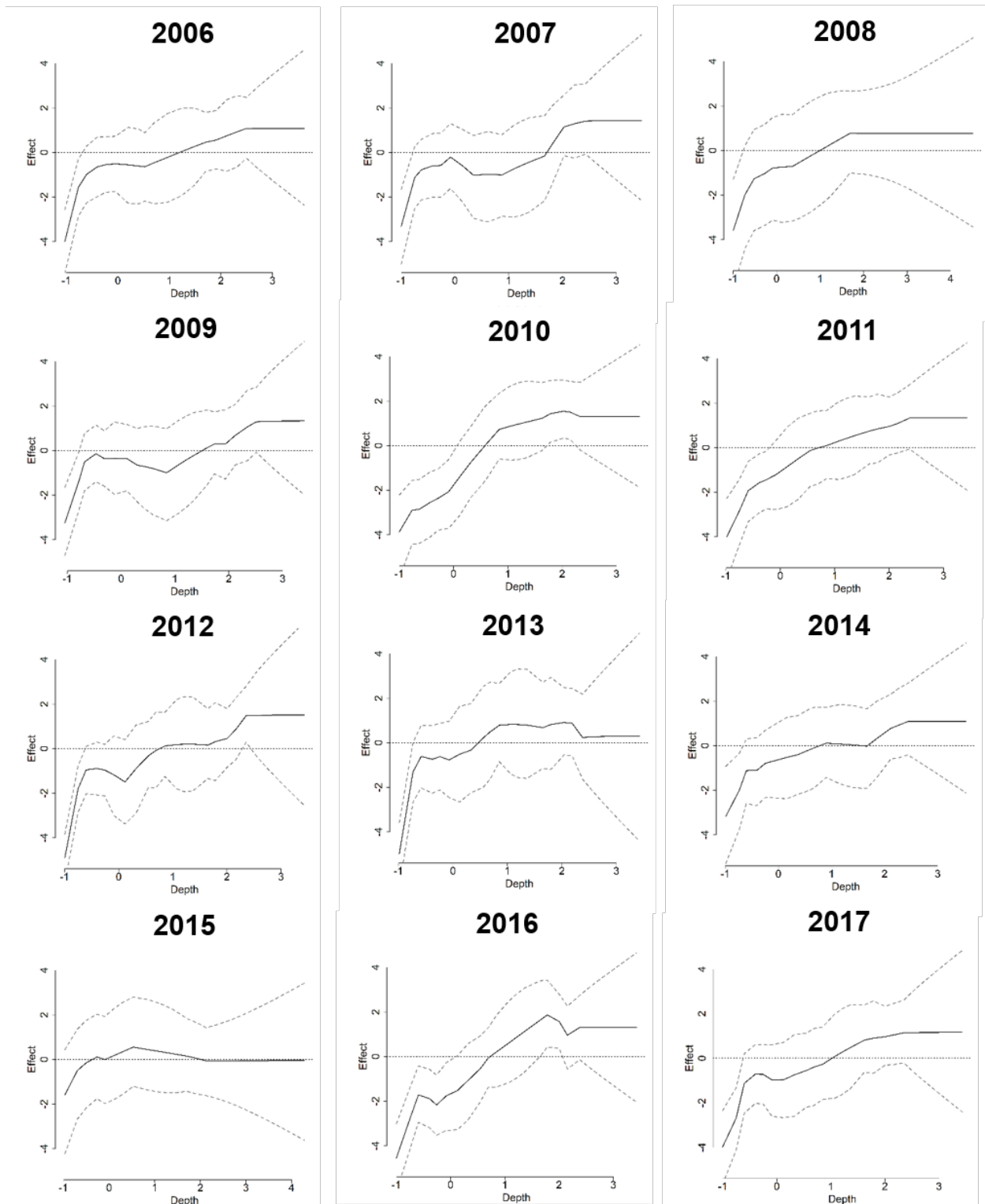


Figure 2. Mean and 95% credible intervals for the posterior distribution of the bathymetry smoothed effect on *Calanus* biomass density in the Gulf of St. Lawrence, Canada in early summer season (June–early July) from 2006 to 2017. Depth values are standardized and range from 0–500m.

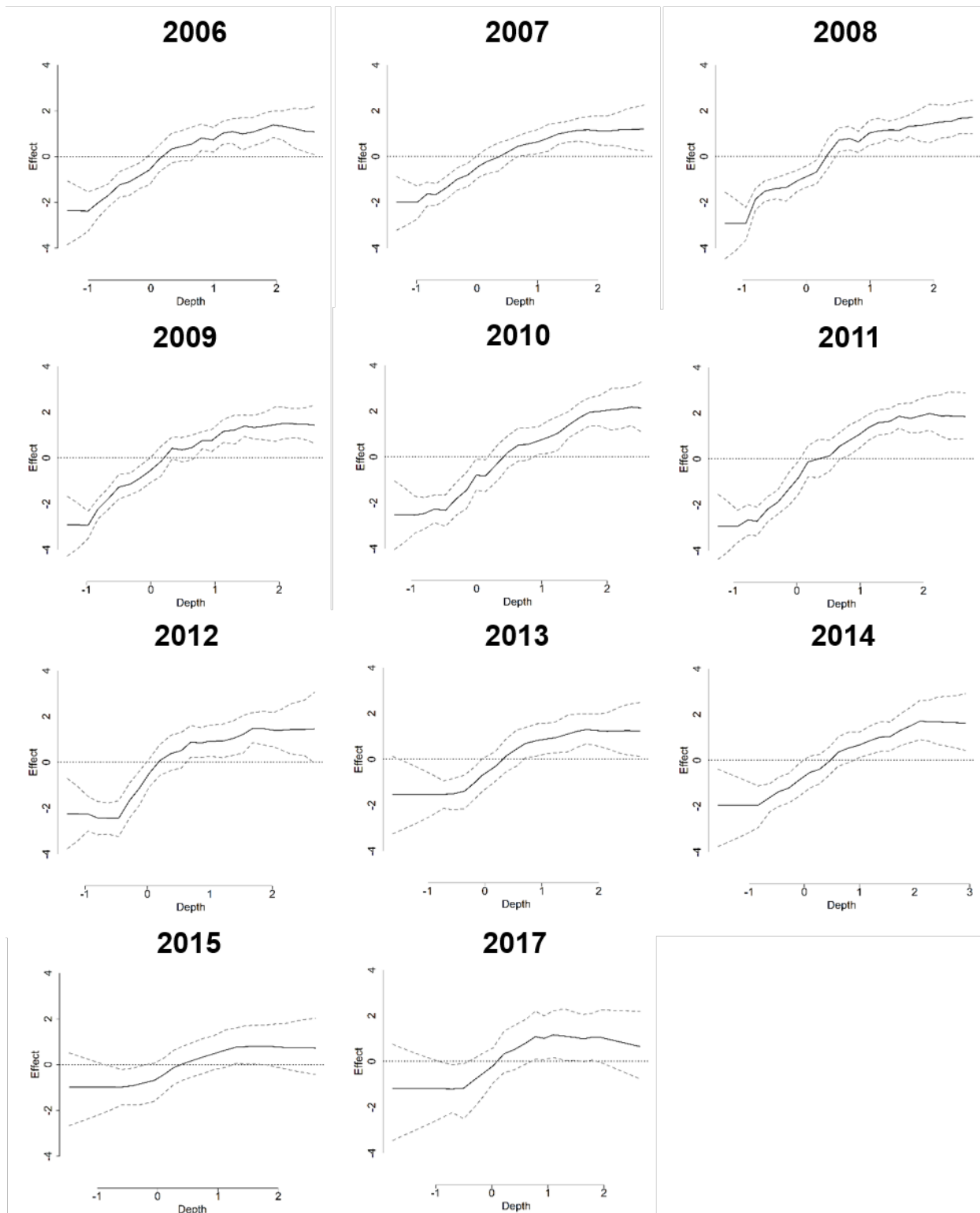


Figure 3. Mean and 95% credible intervals for the posterior distribution of the bathymetry smoothed effect on *Calanus* biomass density in the Gulf of St. Lawrence, Canada in late summer season (late July–September) from 2006 to 2015 and 2017. Depth values are standardized and range from 0–500m.

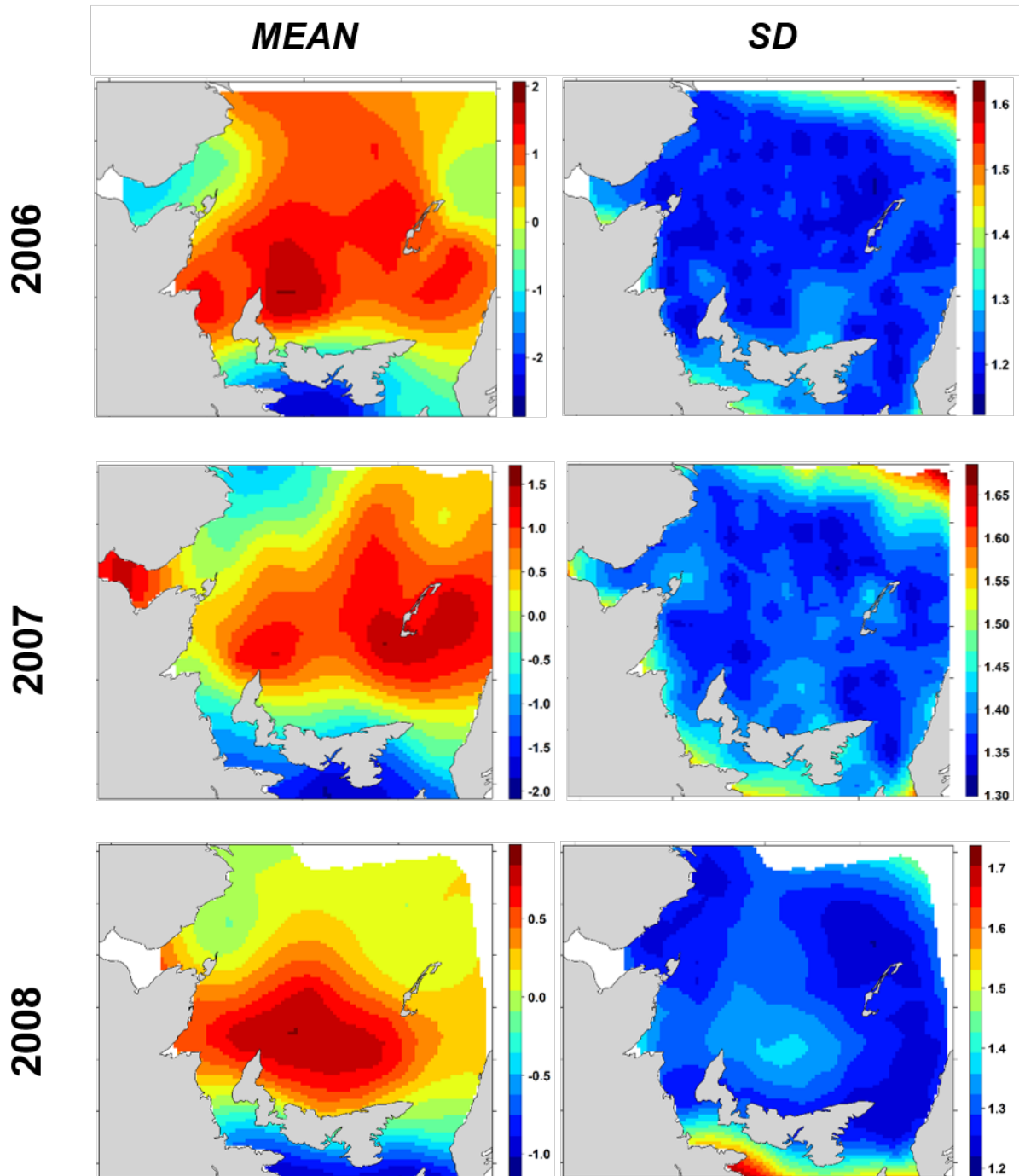


Figure 4. Posterior mean and standard deviation (SD) of the spatial random effect for the model predicting *Calanus* abundance in the Gulf of St. Lawrence, Canada in early season (2006–2008). Note year-specific legend scales to facilitate visual interpretation of spatial random effect each year.

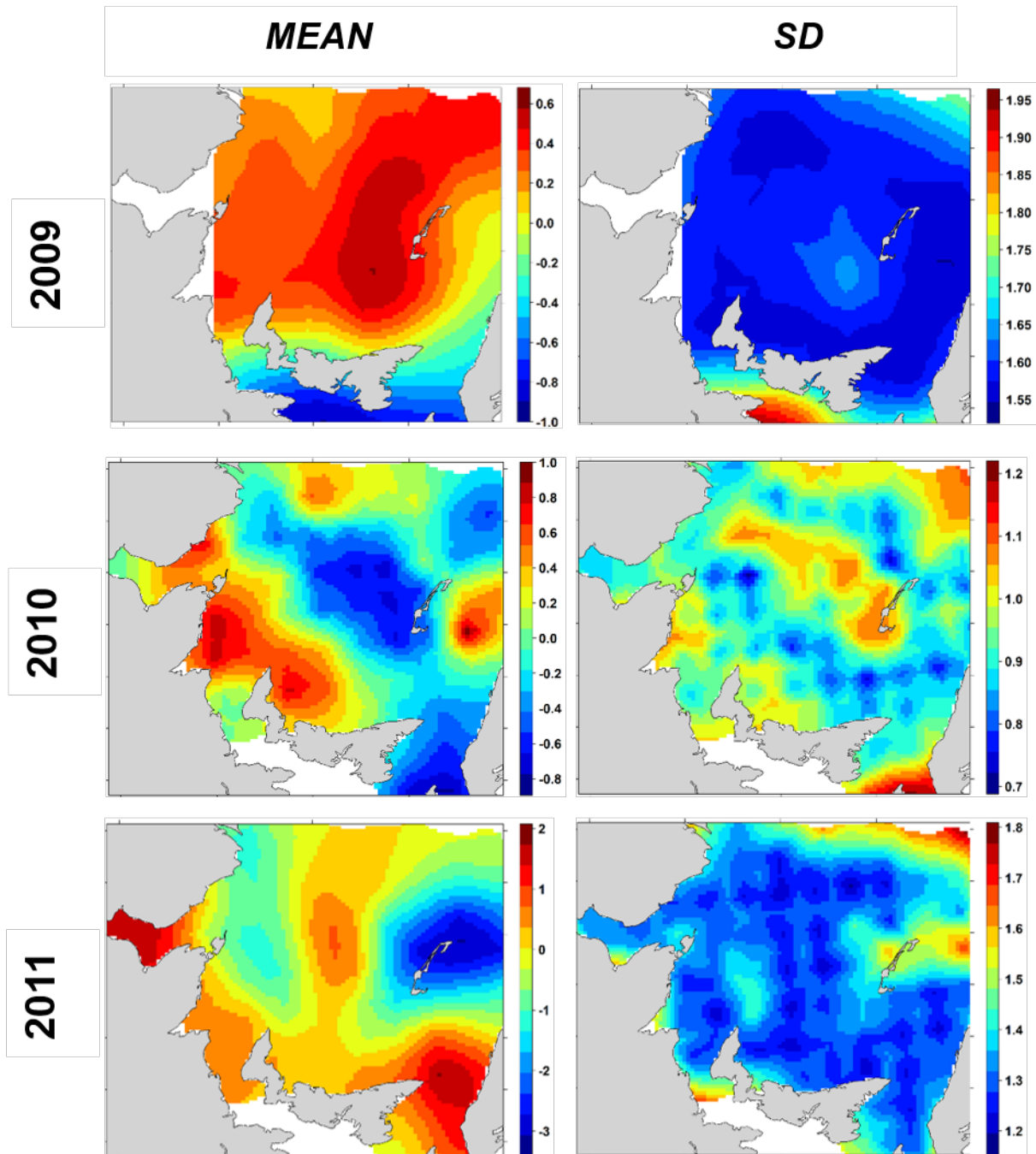


Figure 4 (continued). Posterior mean and standard deviation (SD) of the spatial random effect for the model predicting *Calanus* abundance in the Gulf of St. Lawrence, Canada in early season (2009–2011). Note year-specific legend scales to facilitate visual interpretation of spatial random effect each year.

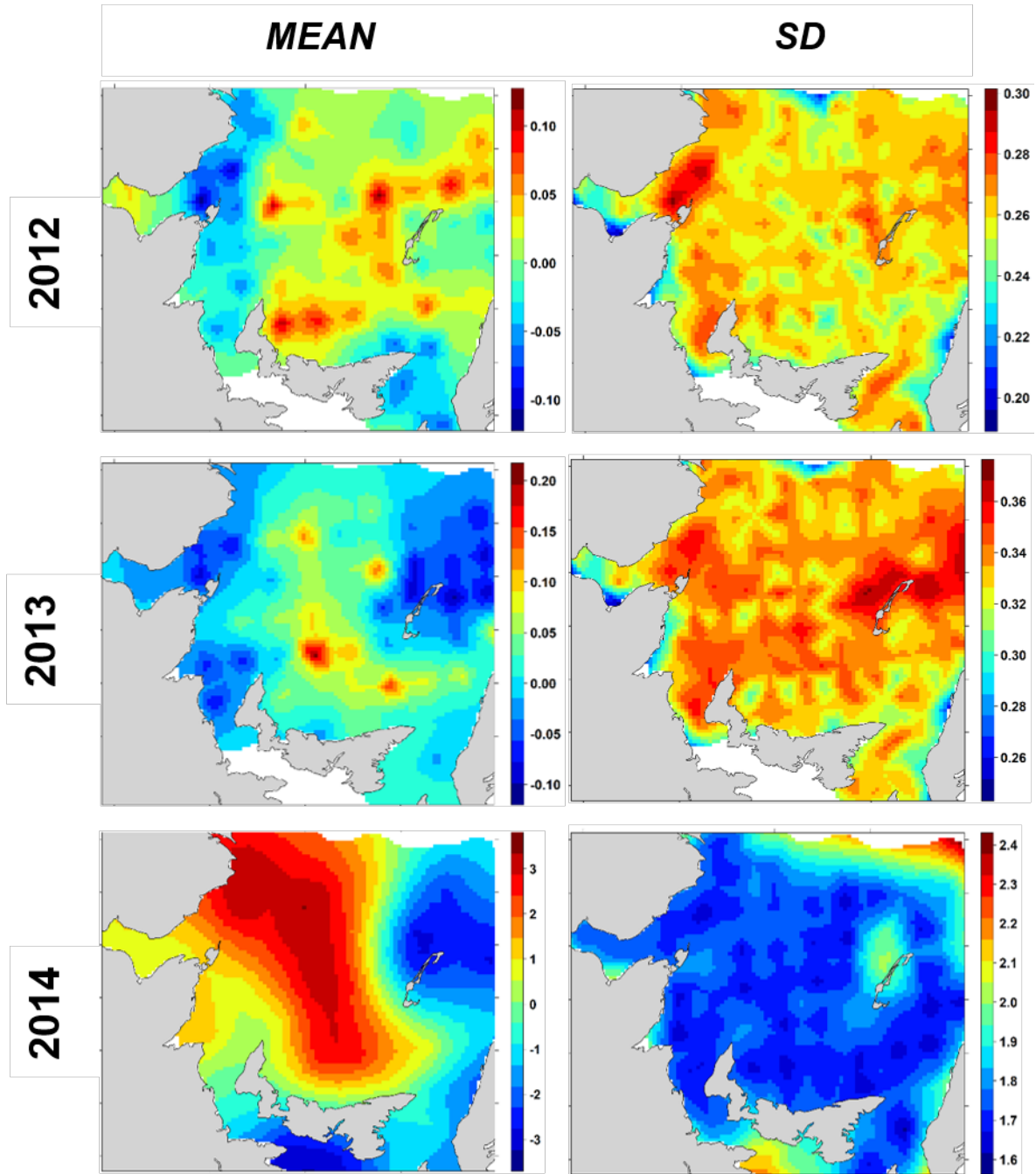


Figure 4 (continued). Posterior mean and standard deviation (SD) of the spatial random effect for the model predicting *Calanus* abundance in the Gulf of St. Lawrence, Canada in early season (2012–2014). Note year-specific legend scales to facilitate visual interpretation of spatial random effect each year.

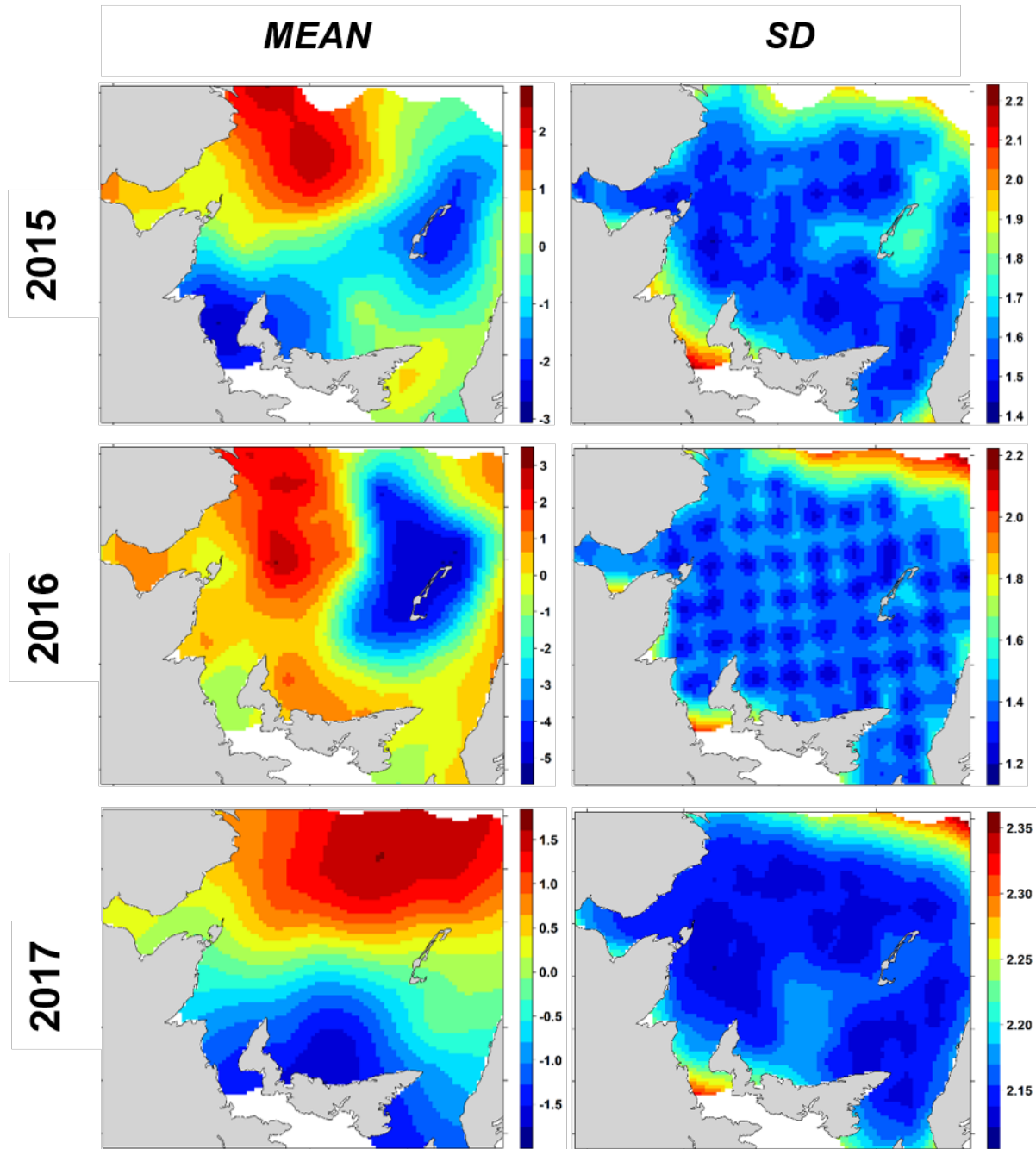


Figure 4 (continued). Posterior mean and standard deviation (SD) of the spatial random effect for the model predicting *Calanus* abundance in the Gulf of St. Lawrence, Canada in early season (2015–2017). Note year-specific legend scales to facilitate visual interpretation of spatial random effect each year.

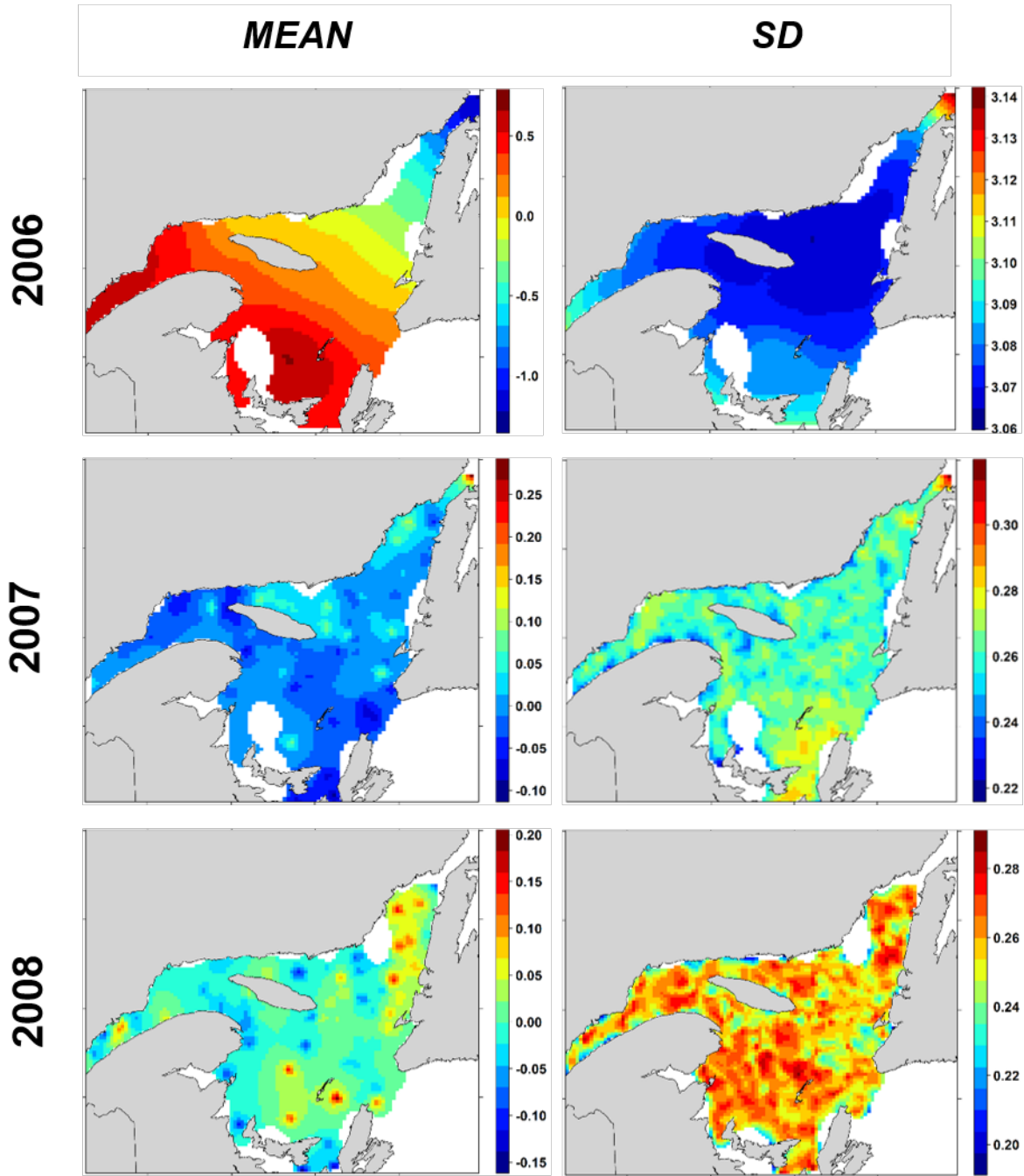


Figure 5. Posterior mean and standard deviation (SD) of the spatial random effect for the model predicting *Calanus* abundance in the Gulf of St. Lawrence, Canada in late season (2006–2008). Note year-specific legend scales to facilitate visual interpretation of spatial random effect each year.

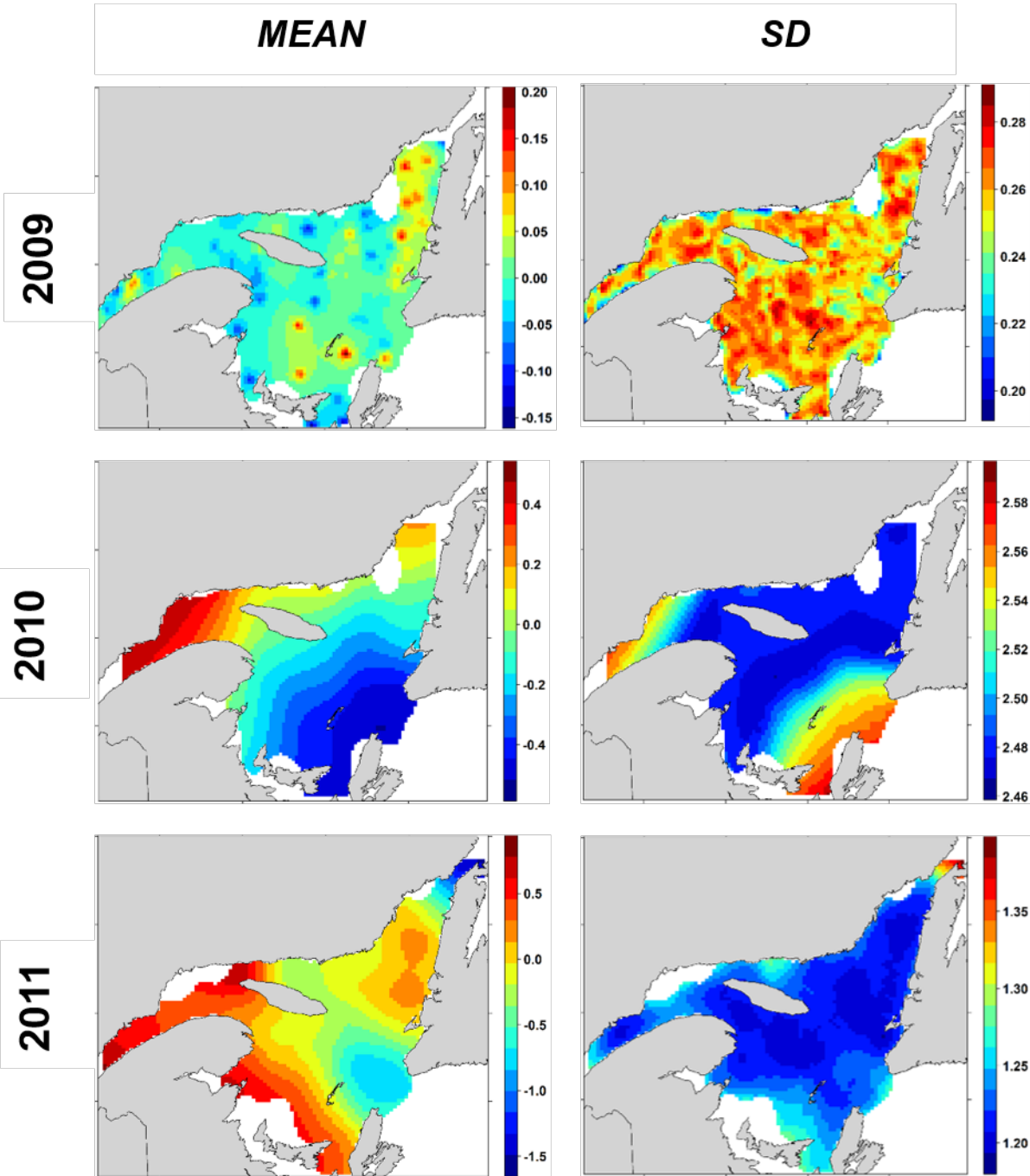


Figure 5 (continued). Posterior mean and standard deviation (SD) of the spatial random effect for the model predicting *Calanus* abundance in the Gulf of St. Lawrence, Canada in late season (2009–2011). Note year-specific legend scales to facilitate visual interpretation of spatial random effect each year.

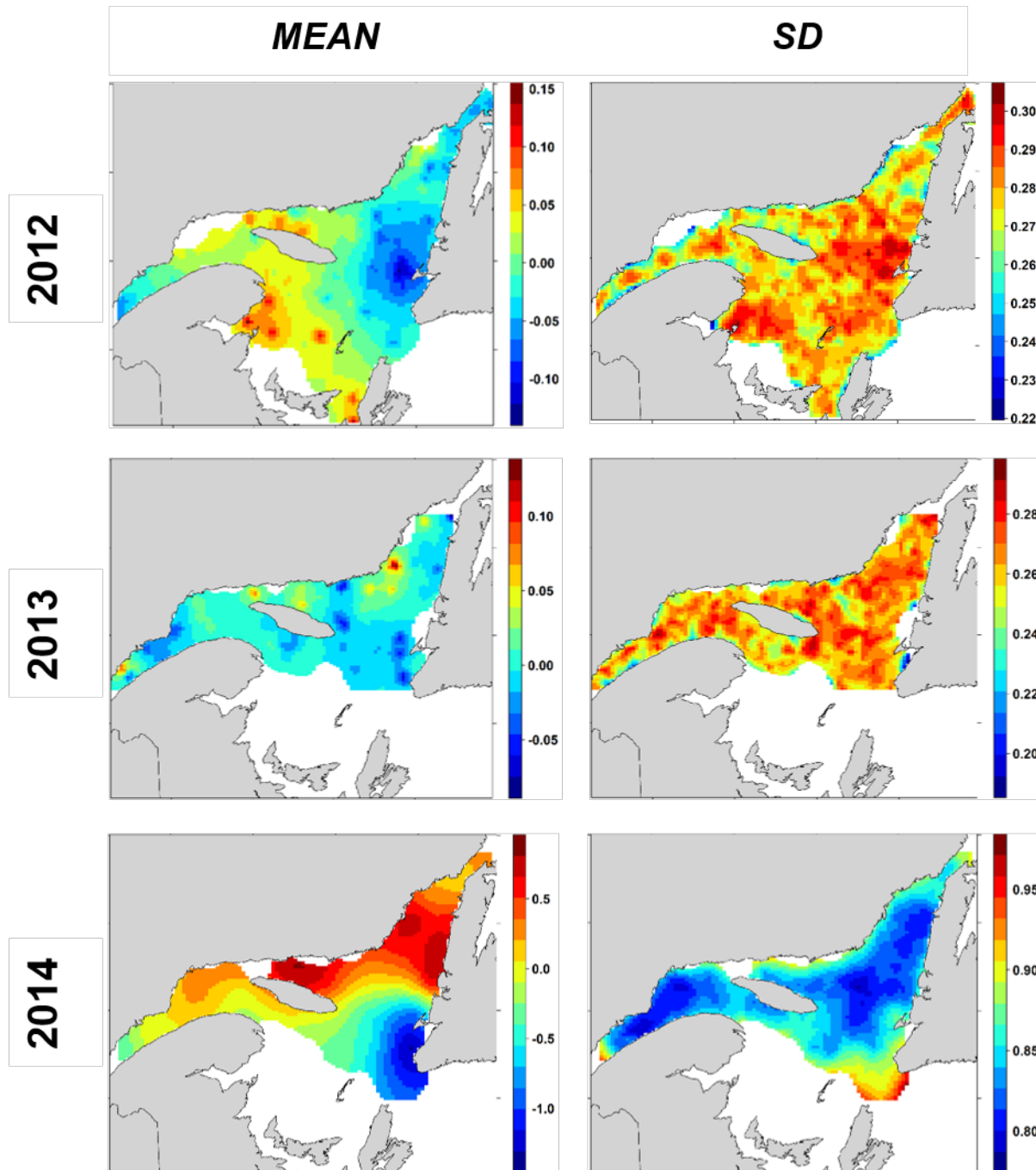


Figure 5 (continued). Posterior mean and standard deviation (SD) of the spatial random effect for the model predicting *Calanus* abundance in the Gulf of St. Lawrence, Canada in late season (2012–2014). Note year-specific legend scales to facilitate visual interpretation of spatial random effect each year.

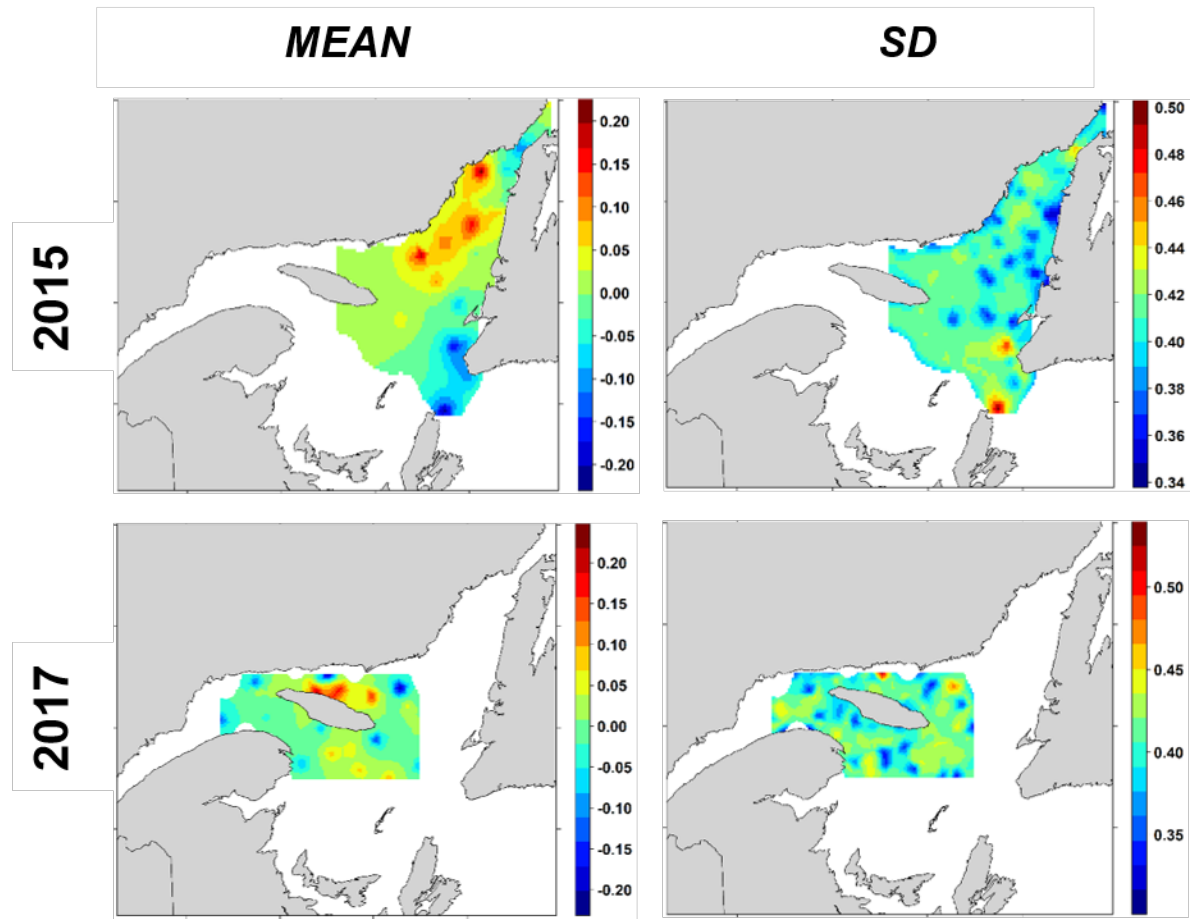


Figure 5 (continued). Posterior mean and standard deviation (SD) of the spatial random effect for the model predicting *Calanus* abundance in the Gulf of St. Lawrence, Canada in late season (2015–2017). Note year-specific legend scales to facilitate visual interpretation of spatial random effect each year.

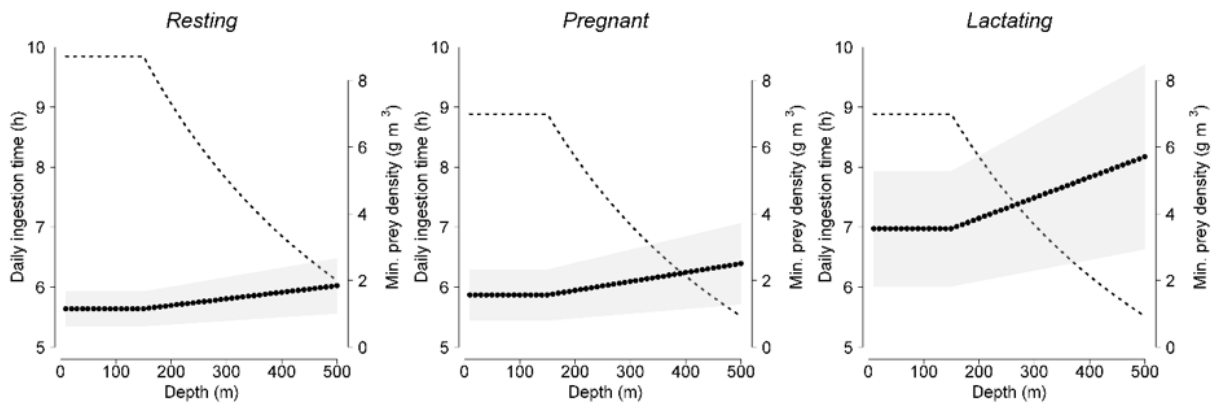


Figure 6. Hypothetical daily prey ingestion time (h; dashed line) and minimum prey (*Calanus*) density requirement (g m^{-3} ; filled black circles) for resting (left), pregnant (middle) and lactating (right) North Atlantic right whales as a function of foraging depth (m). Minimum prey density is defined as the density required to balance daily energy expenditure and is obtained by solving for D_p in the linear E_{in} equation (see Methods). Shaded areas delimit low and high estimates of minimum prey density requirements.

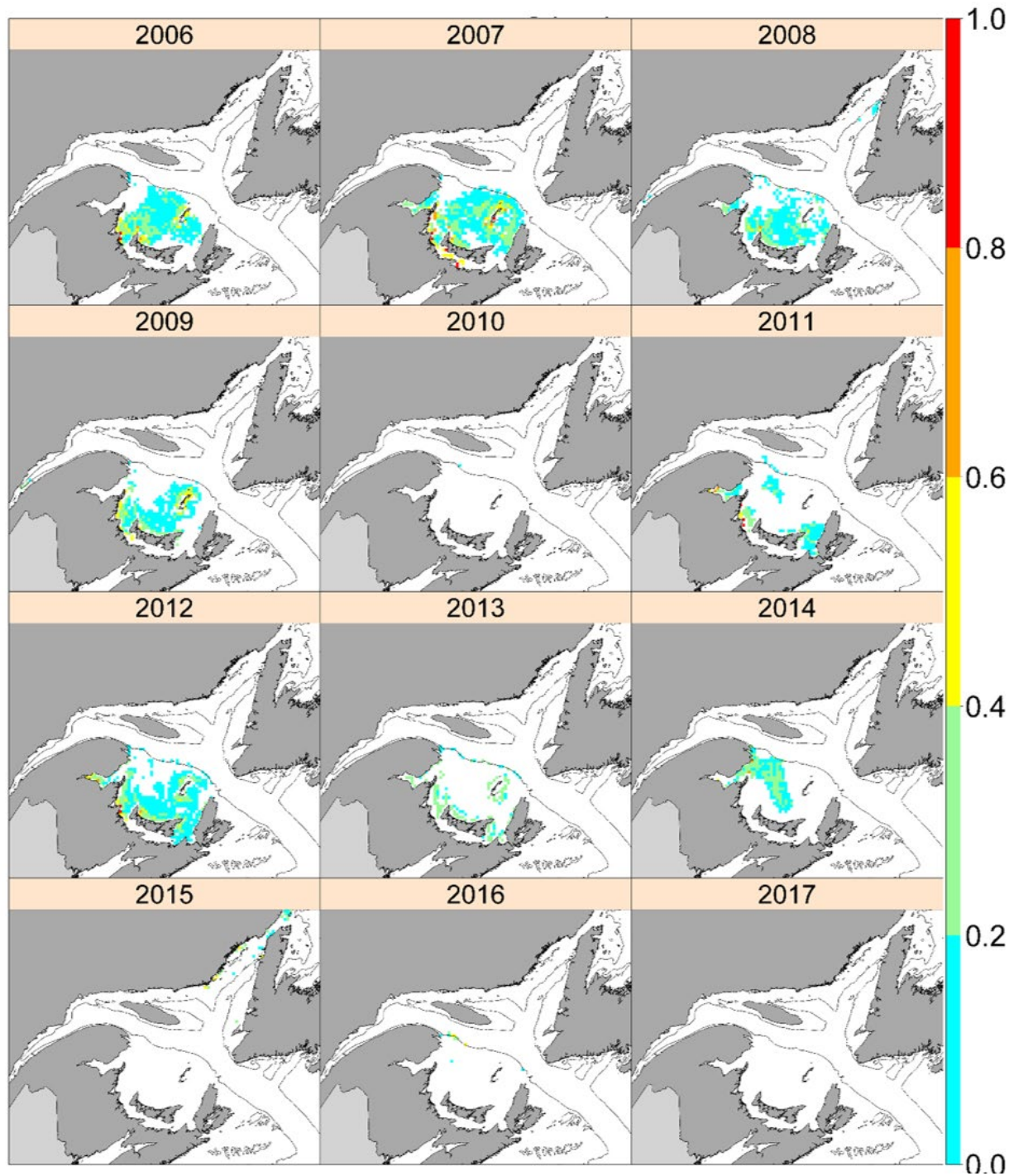


Figure 7. Potential suitable foraging habitat in the Gulf of St. Lawrence from June to September 2006–2017 for **resting** North Atlantic right whales under “**minimum**” energy input and expenditure conditions (see Methods for details). E_{net} values are standardized (0 to 1) by dividing the number of depth layers with $E_{net}>0$ by the total number of depth layers at each grid cell. The 200m isobath is shown. A value of 1.0 signifies that 100% of the water column at a given cell location was predicted to have suitable prey densities.

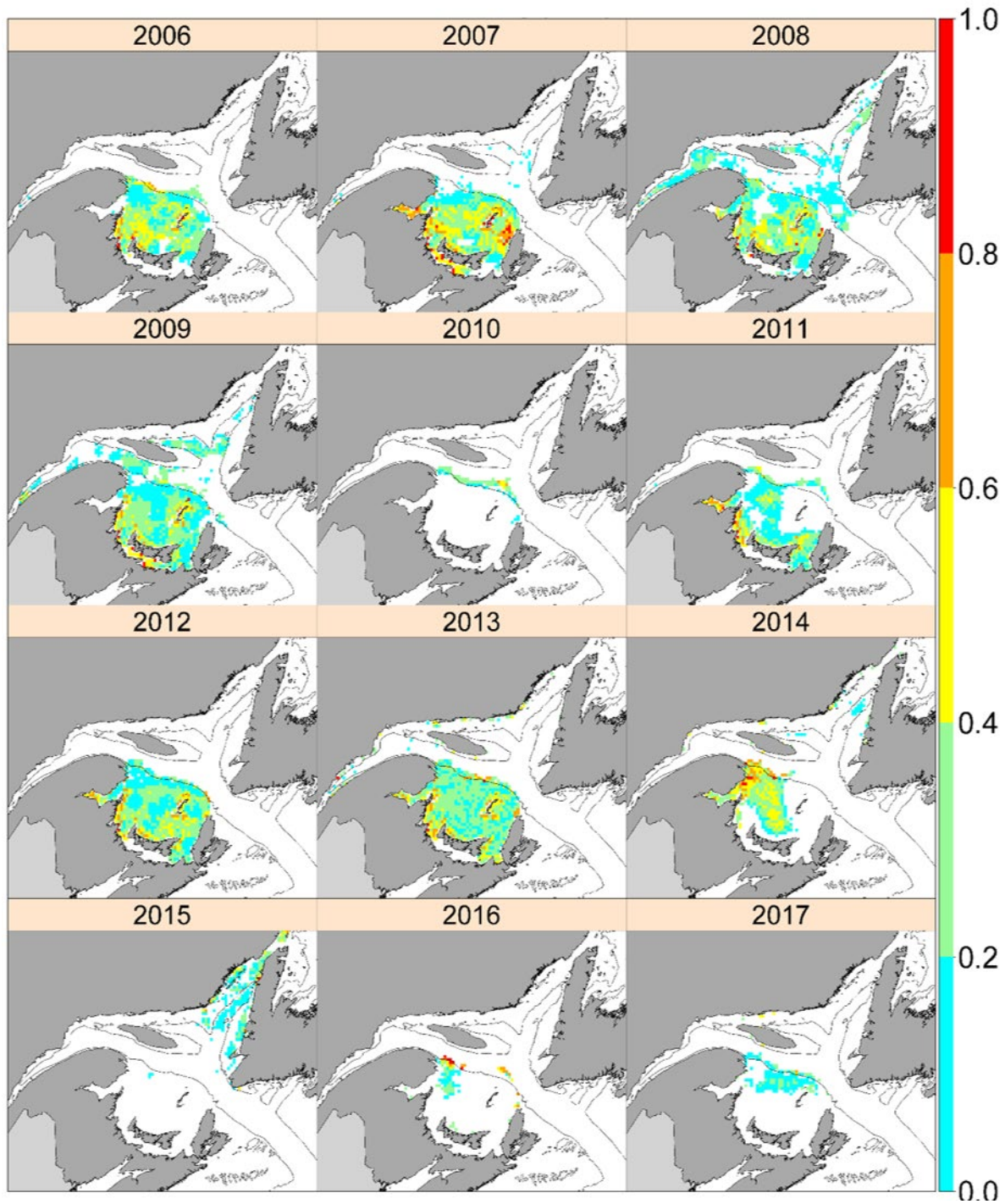


Figure 8. Potential suitable foraging habitat in the Gulf of St. Lawrence from June to September 2006–2017 for **resting** North Atlantic right whales under “**maximum**” energy input and expenditure conditions (see Methods for details). E_{net} values are standardized (0 to 1) by dividing the number of depth layers with $E_{net}>0$ by the total number of depth layers at each grid cell. The 200m isobath is shown.

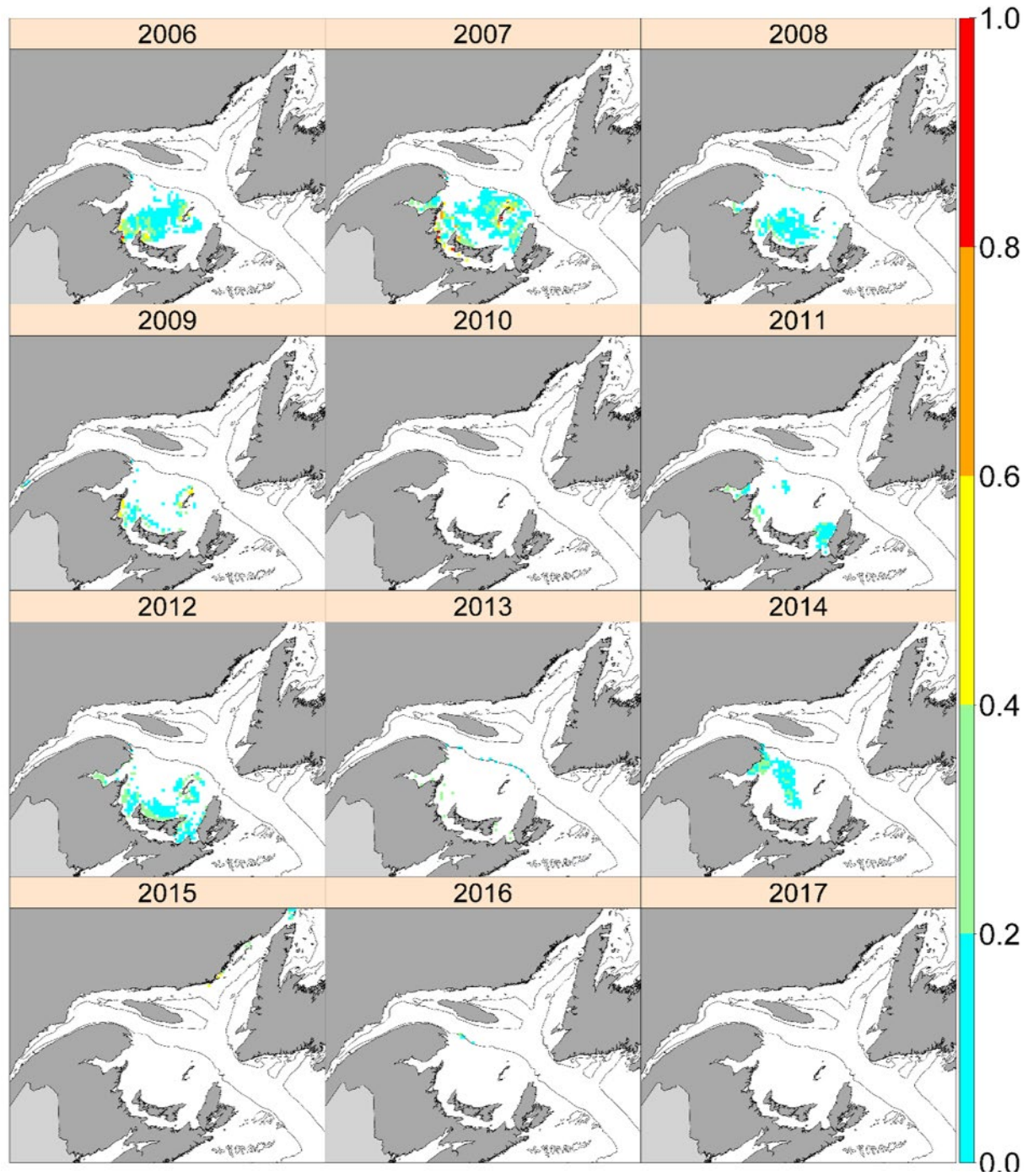


Figure 9. Potential suitable foraging habitat in the Gulf of St. Lawrence from June to September 2006–2017 for **pregnant** North Atlantic right whales under “**minimum**” energy input and expenditure conditions (see Methods for details). E_{net} values are standardized (0 to 1) by dividing the number of depth layers with $E_{net}>0$ by the total number of depth layers at each grid cell. The 200m isobath is shown.

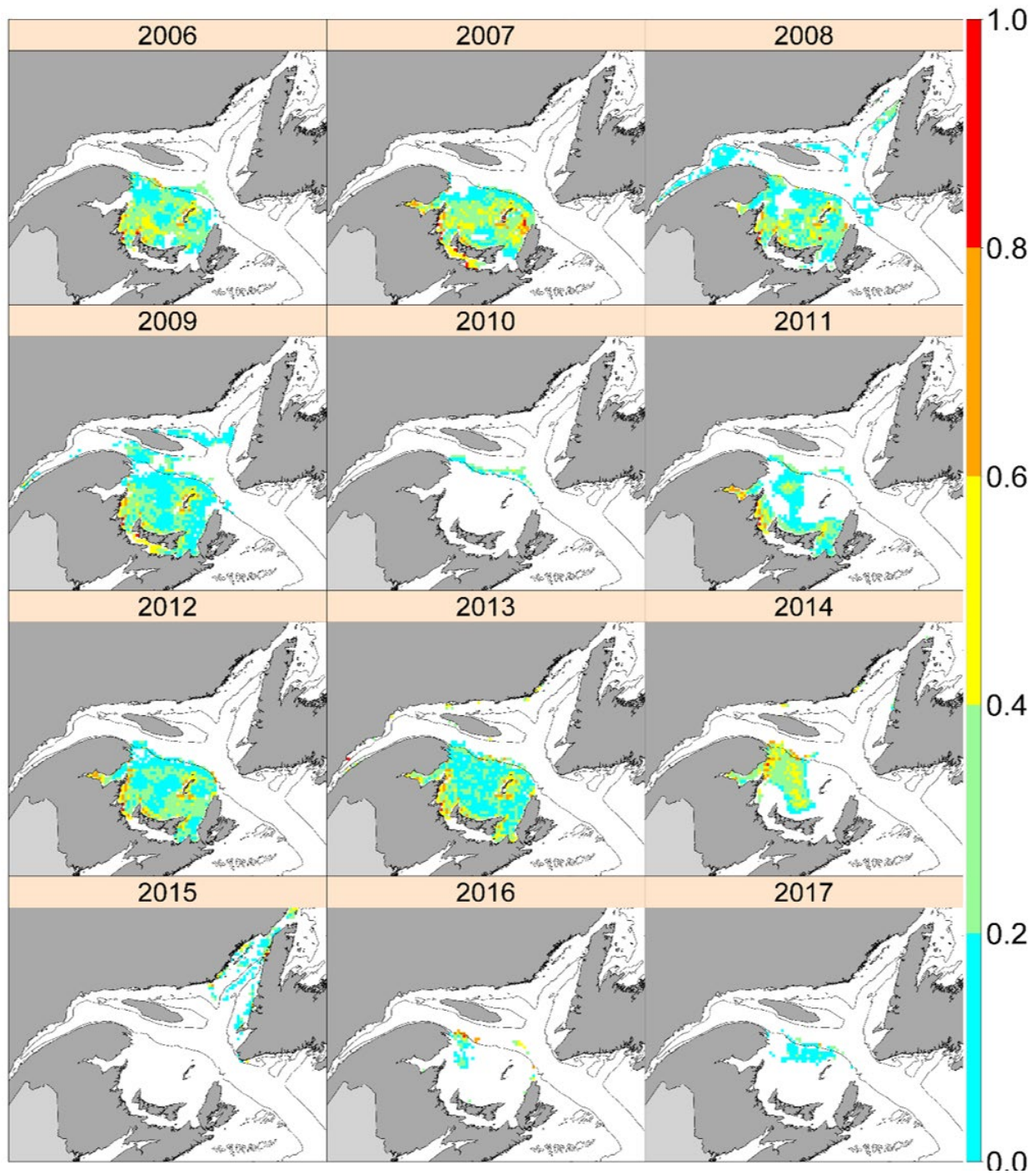


Figure 10. Potential suitable foraging habitat in the Gulf of St. Lawrence from June to September 2006–2017 for **lactating** North Atlantic right whales under “**minimum**” energy input and expenditure conditions (see Methods for details). E_{net} values are standardized (0 to 1) by dividing the number of depth layers with $E_{net}>0$ by the total number of depth layers at each grid cell.

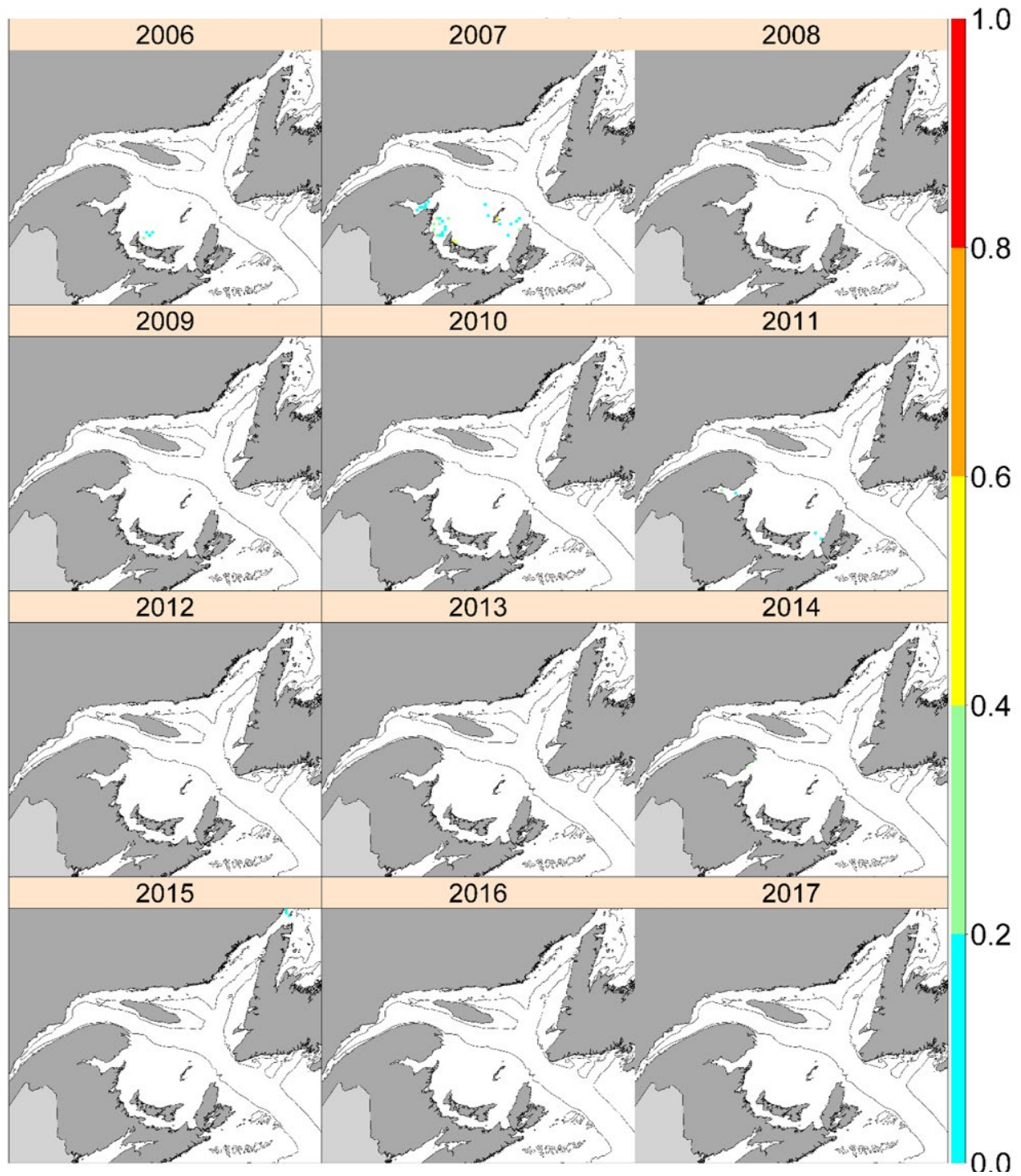


Figure 11. Potential suitable foraging habitat in the Gulf of St. Lawrence from June to September 2006–2017 for **lactating** North Atlantic right whales under “**minimum**” energy input and expenditure conditions (see Methods for details). E_{net} values are standardized (0 to 1) by dividing the number of depth layers with $E_{net}>0$ by the total number of depth layers at each grid cell. The 200m isobath is shown.

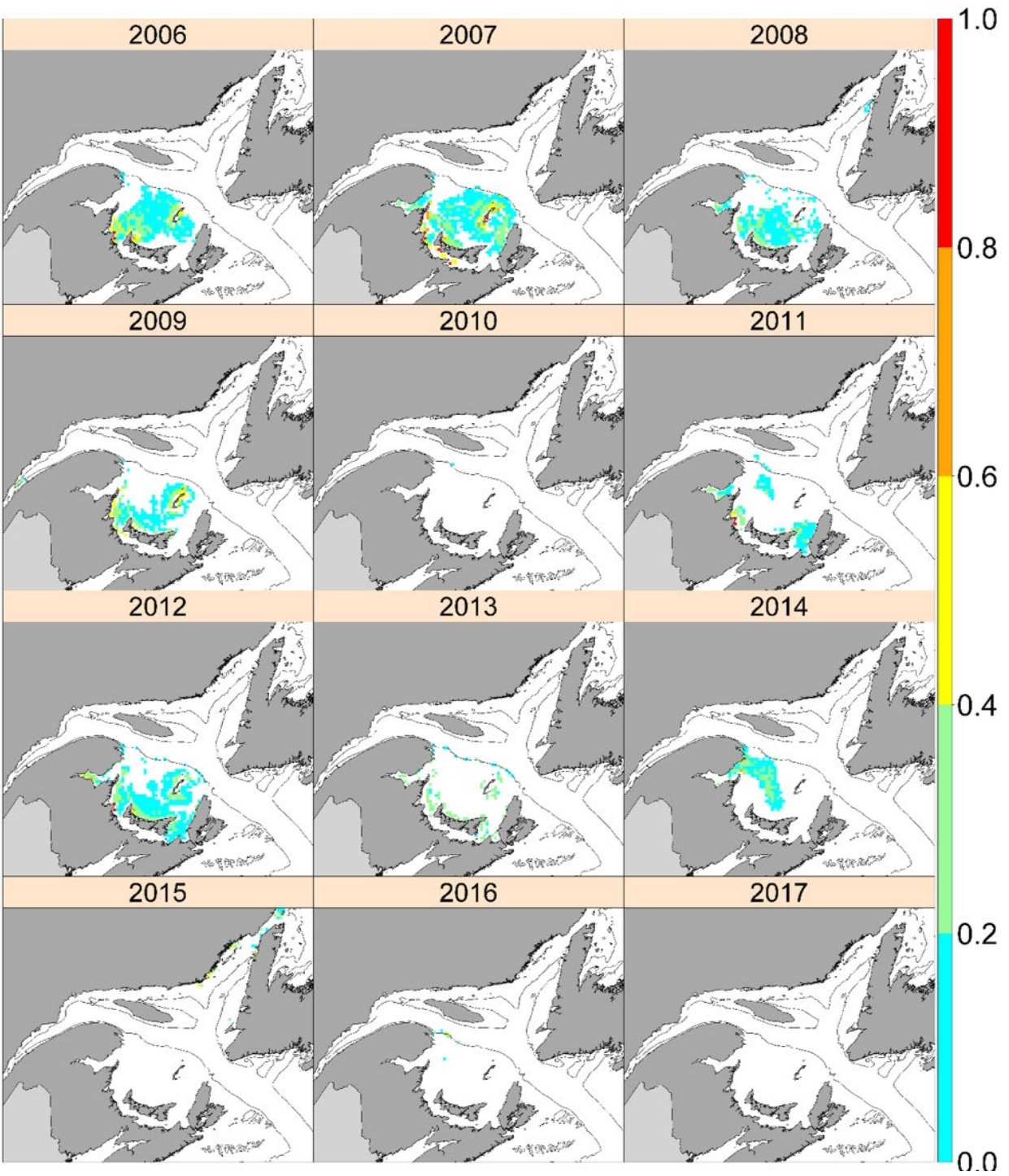


Figure 12. Potential suitable foraging habitat in the Gulf of St. Lawrence from June to September 2006–2017 for **lactating** North Atlantic right whales under “**maximum**” energy input and expenditure conditions (see Methods for details). E_{net} values are standardized (0 to 1) by dividing the number of depth layers with $E_{net}>0$ by the total number of depth layers at each grid cell. The 200m isobath is shown.

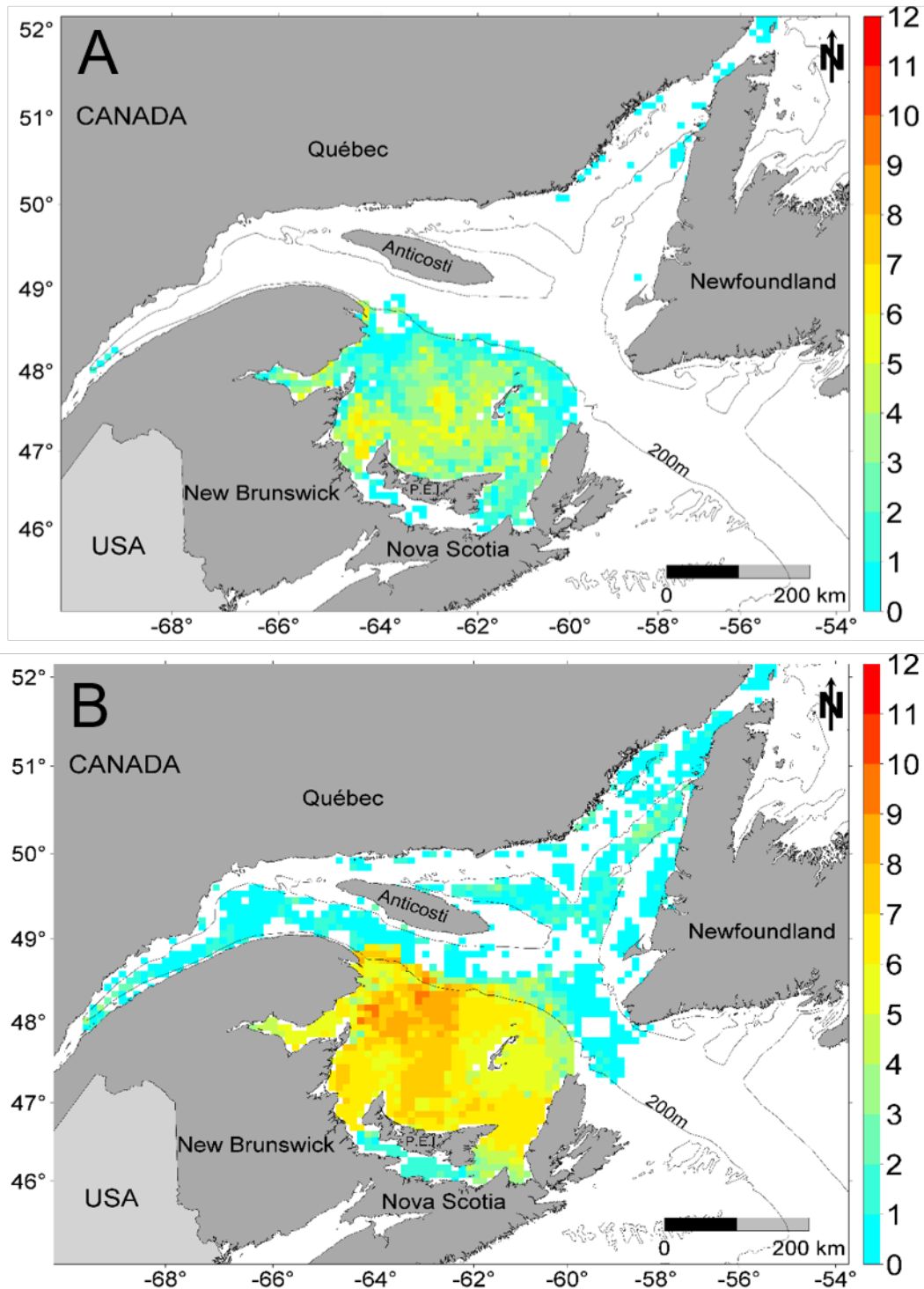


Figure 13. Persistent suitable foraging habitat in the Gulf of St. Lawrence from June to September 2006–2017 for **resting** North Atlantic right whales under minimum (A) and maximum (B) energy input and expenditure conditions (see Methods for details). Scale shows the number of years a given grid cell had at least one depth layer with suitable prey density.

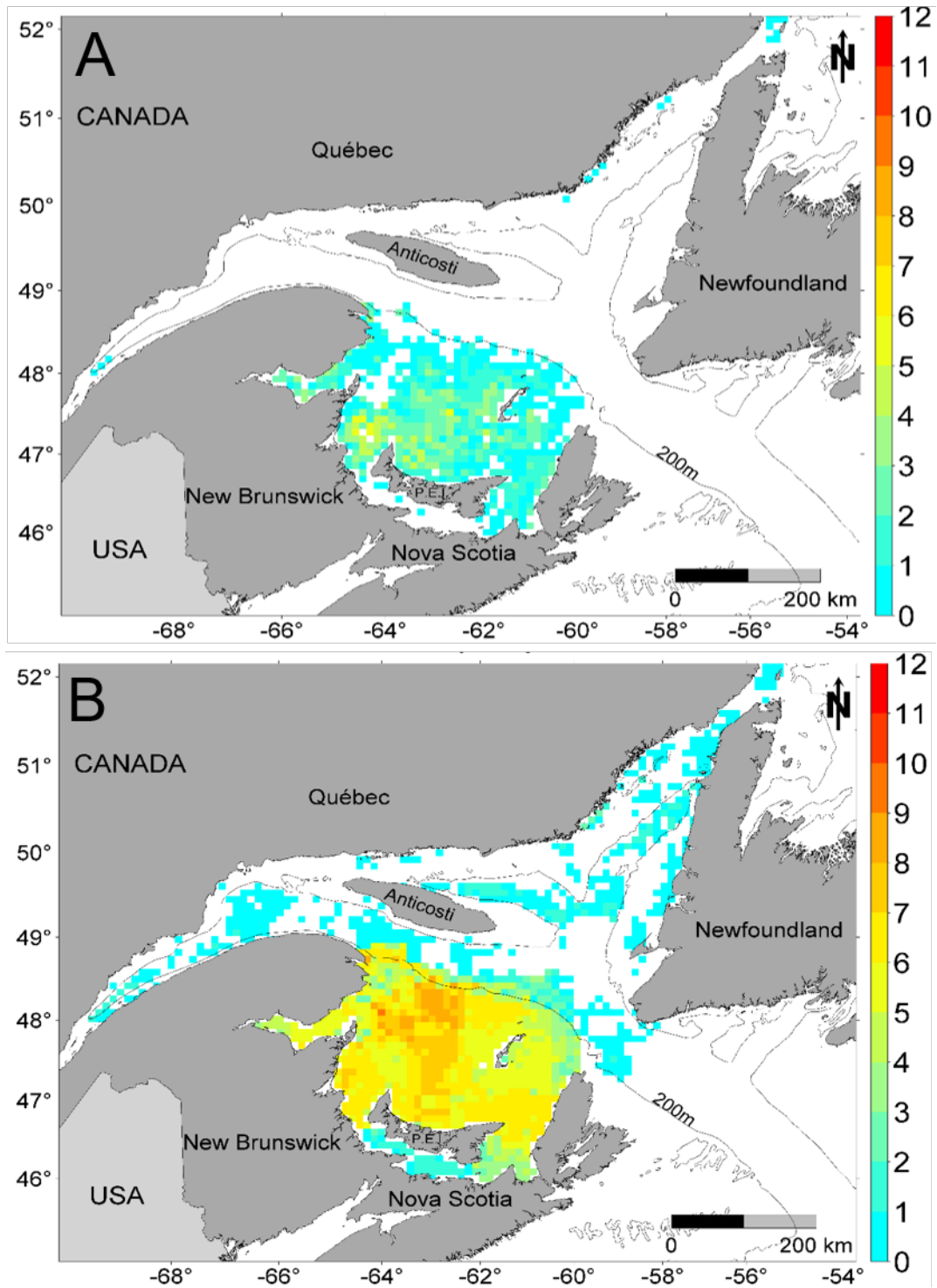


Figure 14. Persistent suitable foraging habitat in the Gulf of St. Lawrence from June to September 2006–2017 for **pregnant** North Atlantic right whales under minimum (A) and maximum (B) energy input and expenditure conditions (see Methods for details). Scale shows the number of years a given grid cell had at least one depth layer with suitable prey density.

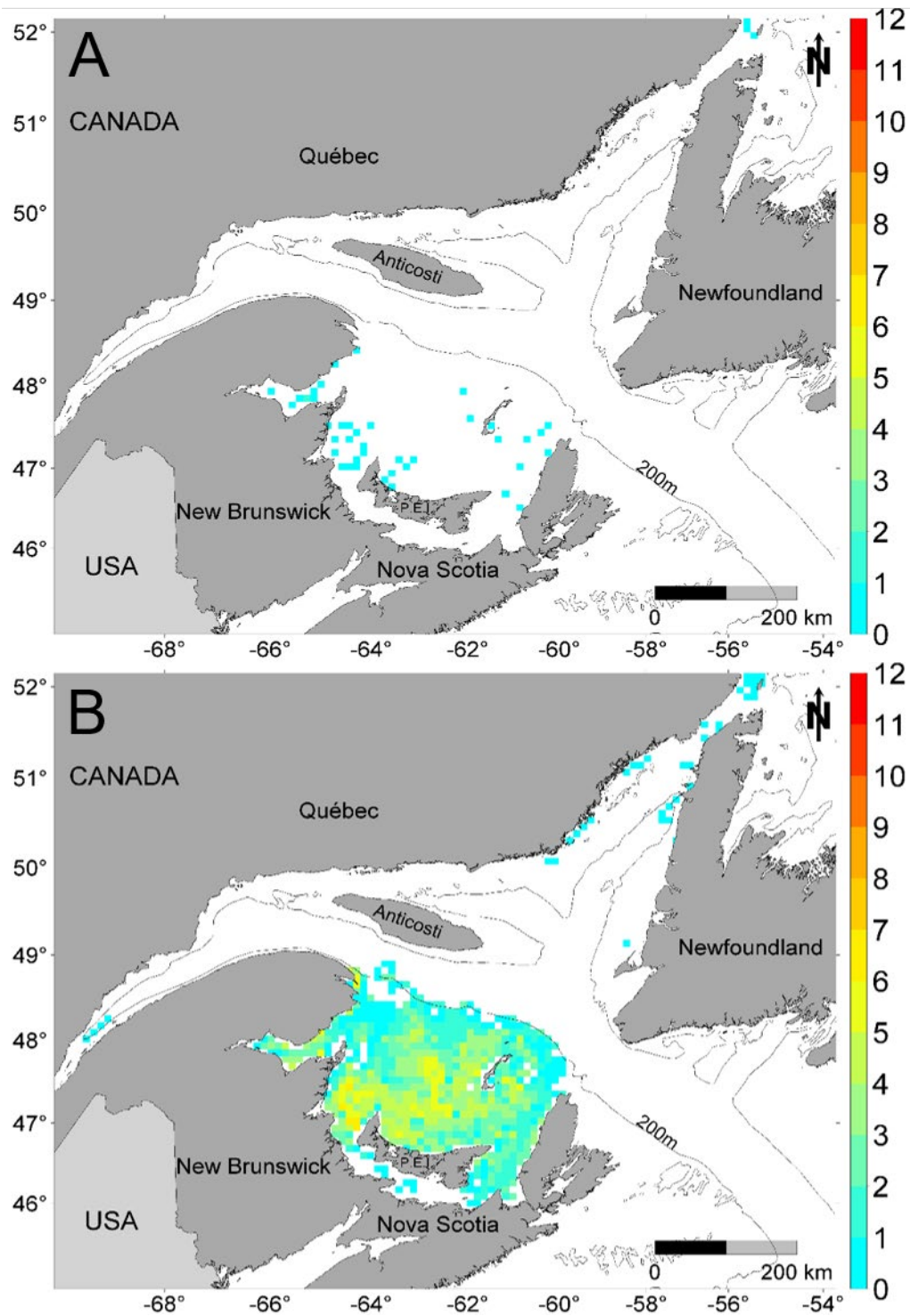


Figure 15. Persistent suitable foraging habitat in the Gulf of St. Lawrence from June to September 2006–2017 for **lactating** North Atlantic right whales under minimum (A) and maximum (B) energy input and expenditure conditions (see Methods for details). Scale shows the number of years a given grid cell had at least one depth layer with suitable prey density.

APPENDIX

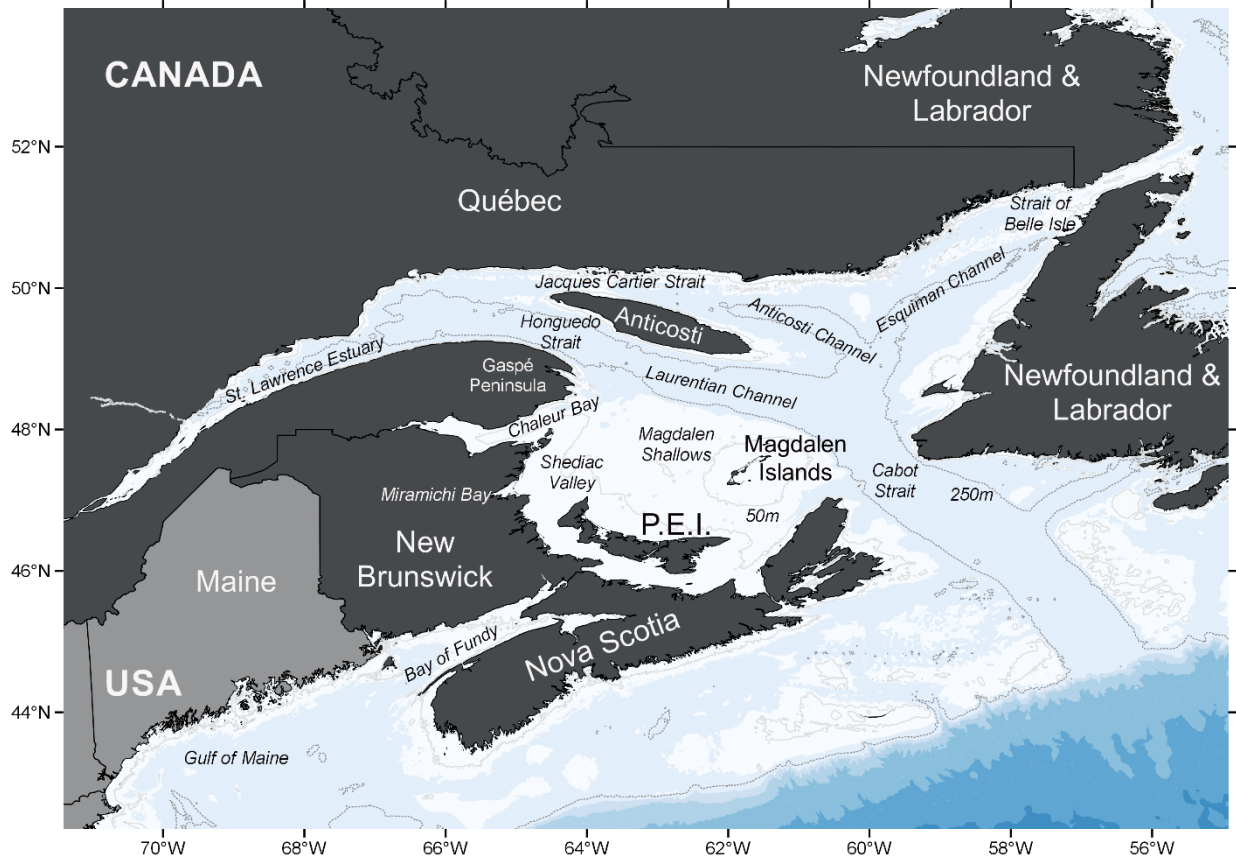


Figure S1. Map of the Estuary and Gulf of St. Lawrence, Canada.